DEFORMATION ANALYSIS OF FUNCTIONALLY GRADED TUBES UNDER PRESSURE

A THESIS SUBMITTED TO

THE GRADUATE SCHOOL OF NATURAL AND APPLIED SCIENCES

OF

ATILIM UNIVERSITY

BY

ÖMÜR EREN

IN PARTIAL FULFILLMENT OF THE REQUIREMENTS FOR THE DEGREE OF

MASTER OF SCIENCE

IN

THE DEPARTMENT OF CIVIL ENGINEERING

NOVEMBER, 2009

Approval of the Graduate School of Natural and Applied Sciences, Atılım University.

_____

Prof. Dr. İbrahim AKMAN
Director

I certify that this thesis satisfies all the requirements as a thesis for the degree of Master of Science.

_____

Asst. Prof. Dr. Cumhur Aydın
Head of Department

This is to certify that we have read the thesis "Deformation Analysis of Functionally Graded Tubes Under Pressure" submitted by Ömür EREN and that in our opinion it is fully adequate, in scope and quality, as a thesis for the degree of Master of Science.

_____

Asst. Prof. Dr. Tolga Akış
Supervisor

Examining Committee Members

Asst. Prof. Dr. Hakan Argeşo _____
Manuf. Eng. Dept., Atılım University

Asst. Prof. Dr. Tolga Akış _____
Civil Eng. Dept., Atılım University

Asst. Prof. Dr. Eray Baran _____
Civil Eng. Dept., Atılım University

Date: November 12, 2009

I declare and guarantee that all data, knowledge and information in this document has been obtained, processed and presented in accordance with academic rules and ethical conduct. Based on these rules and conduct, I have fully cited and referenced all material and results that are not original to this work.

Name, Last name: Ömür Eren

Signature:

ABSTRACT

DEFORMATION ANALYSIS OF FUNCTIONALLY GRADED TUBES UNDER PRESSURE

Eren, Ömür

M.S., Civil Engineering Department

Supervisor: Asst. Prof. Dr. Tolga Akış

November 2009, 57 pages

The purpose of this study is to investigate the elastic behaviour of the functionally graded tubes under internal or external pressure. The modulus of elasticity and the uniaxial yield limit of the tube material are assumed to vary nonlinearly in the radial direction. In the framework of small deformations and a state of plane strain, the expressions of stresses and displacement are obtained analytically. In addition, the yielding behaviour of the functionally graded tubes with (a) free ends under internal pressure, (b) free ends under external pressure, (c) fixed ends under internal pressure, and (d) fixed ends under external pressure are examined using von Mises yield criterion. Using the analytical expressions, various numerical examples are handled and the effect of the functionally graded material (FGM) parameters on the elastic limit pressure is shown.

Keywords: Stress analysis; Functionally graded materials; von Mises yield criteria

ÖZ

BASINÇ ETKİSİ ALTINDAKİ FONKSİYONEL DERECELENDİRİLMİŞ MALZEMEDEN YAPILMIŞ TÜPLERİN DEFORMASYON ANALİZİ

Eren, Ömür

Yüksek Lisans, İnşaat Mühendisliği Bölümü

Tez Yöneticisi: Yrd. Doç. Dr. Tolga Akış

Kasım 2009, 57 sayfa

Bu çalışmanın amacı, fonksiyonel derecelendirilmiş malzemeden yapılmış tüplerin iç veya dış basınç altındaki elastik davranışını incelemektir. Tüp malzemesinin elastik modülünün ve eksenel akma limitinin radyal yönde, doğrusal olmayan bir şekilde değiştiği varsayılmıştır. Basınç altındaki tüplere ait gerilme ve yer değiştirme ifadeleri düzlemsel şekil değiştirme ve deformasyonların küçük olduğu varsayımları göz önünde bulundurularak analitik olarak elde edilmiştir. Bunlara ek olarak, von Mises akma kriteri kullanılarak fonksiyonel derecelendirilmiş tüplerin akma davranışı (a) uçları eksenel yönde serbest-iç basınç, (b) uçları eksenel yönde serbest-dış basınç, (c) uçları eksenel yönde sabitlenmiş-iç basınç ve (d) uçları eksenel yönde sabitlenmiş-dış basınç durumları için ayrı ayrı incelenmiştir. Bulunan analitik ifadeler kullanılarak bazı sayısal örnekler ele alınmış, fonksiyonel

derecelendirme parametrelerinin elastik limit akma basıncına etkileri gösterilmiştir.

Anahtar Kelimeler: Gerilme analizi; Fonksiyonel derecelendirilmiş malzemeler; von Mises akma kriteri

To My Family

ACKNOWLEDGEMENTS

I express sincere appreciation and thanks to my supervisor Asst. Prof. Dr. Tolga Akış for his guidance, insight, and endless patience throughout the research. To my wife, Seçil, I offer sincere thanks for her continuous encouragement and patience during this period. And to my parents and my brother, Onur, who gave their love and support for my whole life.

TABLE OF CONTENTS

LIST OF FIGURES

FIGURES

LIST OF SYMBOLS

r, θ, z	cylindrical polar coordinates
a, b	inner and outer radii of the tube
$\bar{a}, \bar{b}$	dimensionless inner and outer radii of the tube
C_i	integration constants
E	modulus of elasticity
ν	Poisson's ratio
u	radial displacement
$\bar{u}$	dimensionless radial displacement
$\in_i$	strain components
ϕ	non-dimensional stress variable
σ_i	stress components
$\bar{\sigma}_i$	dimensionless stress components
σ_0, σ_Y	initial and subsequent yield stress
σ_C	reference value of uniaxial yield limit
n, m	functionally graded material parameters
$\bar{P}_e$	dimensionless elastic limit pressure

CHAPTER I

INTRODUCTION

Traditional engineering materials have several disadvantages especially at high temperatures and high pressures. For example, due to the mismatch in the thermal expansion coefficients of such materials, higher thermal stresses occur which can cause cracks. The technology leads to a great demand for advanced high performance materials, which can carry higher loads, stand up to high temperatures and corrosive environments. For this reason, a new material system called as functionally graded materials (FGM) was developed. The non-homogeneous structure of an FGM is shown in Fig. 1.1. Nowadays, the studies on the structural elements made of functionally graded materials gathers extensive interest due to the increasing usage in industrial applications.

Details of the production of FGM materials can be found in the study of several researchers. Rooney and Ferrari [1] stated that the concept of functionally graded materials was first suggested by Niino and co-workers at the National Aerospace Laboratory in Japan. Watanabe et al. [2] studied the use of a functionally graded material in the manufacture of a graded permittivity element. Katakam et al. [3] investigated microwave processing of functionally graded bioactive materials. Noguchi et al. [4] studied trial manufacture of functionally graded Si-Ge thermoelectric material. Esteban et al. [5] investigated the FGM material which is fabricated starting from coarse commercial metal powder by a wet processing method. The process presented by Kobayasi [6] is the fabrication of PSZ-SUS 304, which is an FGM.

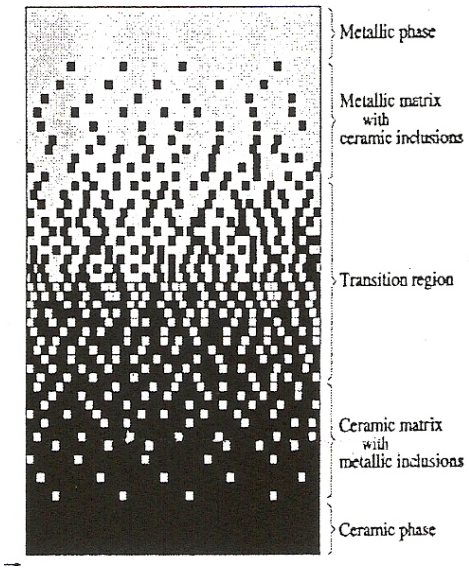

Figure 1.1 Schematic illustration of an FGM with continuously graded microstructure [7]

As observed from the studies given above, there are several different FGM processing methods. Among them, the most common methods can be listed as [8]:

1. Constructive processes:
    a. Powder densification processes
    b. Coating processes
    c. Lamination processes

2. Transport–based processes:
    a. Mass transport processes
    b. Thermal processes
    c. Settling and centrifugal separation processes
    d. Infiltration, macro segregation and Darcian flow processes

On the other hand, a significant number of theoretical studies are performed on the deformation behaviour of functionally graded structural elements. Among them, Eslami et al. [9] investigated the thermal and mechanical stresses in a hollow thick sphere made of functionally graded material. In their study, the material properties are assumed to be graded along the radial direction according to a power law function. The stresses are obtained through the direct method of solution of the Navier equation.

Akış and Eraslan [10] investigated the elastic, partially plastic and fully plastic deformation behavior of rotating FGM hollow shafts with fixed ends. They found that the plastic deformation may commence at the inner or outer surface or even simultaneously at both surfaces. Dai et al. [11] studied the magneto-elastic behavior of FGM cylindrical and spherical vessels placed in a uniform magnetic field which are subjected to internal pressure.

Zhifei et al. [12] studied two different kinds of heterogeneous elastic hollow cylinders. One is a cylinder with multi-layers and another is a cylinder with continuously graded properties. In their study, a new method is presented in order to find the exact solutions of a N-layered elastic hollow cylinder submitted to uniform pressures at the inner and outer surfaces. Shao [13] investigated the thermal/mechanical stresses in a functionally graded circular hollow cylinder. The cylinder that is studied has a finite length which is subjected to axisymmetric thermal and mechanical loads.

Zimmerman [14] studied the thermal stresses and thermal expansion in a uniformly heated functionally graded cylinder. The exact solution is derived for the cylinder whose elastic modulus and thermal expansion coefficient vary linearly with radius.

Akış and Eraslan [15] obtained the plane strain analytical solutions to functionally graded elastic and elastic–plastic pressurized tube problem. It is shown in that study that the elastoplastic response of the functionally graded pressurized tube is affected significantly by the material nonhomogeneity and different modes of plasticization may take place unlike the homogeneous case. Oral and Anlas [16] investigated the

stress distribution in a nonhomogeneous anisotropic cylindrical body in terms of stress potentials where elastic properties change in radial direction.

You et al. [17] presented a method to carry out elastic analysis of thick-walled spherical pressure vessels subjected to internal pressure. Two kinds of pressure vessel are considered in their study: one consists of two homogeneous layers near the inner and outer surfaces of the vessel and one functionally graded layer in the middle; the other consists of the functionally graded material only.

In addition to the studies mentioned above, Shen [18] studied on the nonlinear analysis of FGM plates and shells. Çetin [7] developed the analytical solution of a crack problem in radially graded FGM. Delale and Erdoğan [19] investigated the crack problem of an infinite nonhomogeneous plate with the elastic properties varying in the direction parallel to the crack. Akış [20] studied the elastoplastic analysis of functionally graded spherical pressure vessels under internal pressure.

There are also several studies in the literature that investigate the homogenous pressurized tubes. Among them, Akış and Eraslan [21] studied tightly fitted long concentric tubes, subject to either internal or external pressure with axially constrained ends. Making use of von Mises yield criterion, the critical values of pressure leading to plastic flow are determined in that study.

Yielding of pressurized two-layer shrink-fitted composite tubes with axially constrained ends is investigated in detail by Akış and Eraslan [22]. They found that yielding may begin at the inner tube or at the outer tube or simultaneously in both tubes.

Eraslan and Apatay [23] obtained the analytical solution of a nonlinear strain hardening preheated tube subjected to internal pressure. The solution of the problem is obtained by using incremental theory of plasticity, Tresca's yield criterion and the associated flow rule.

The aim of this study is to obtain the analytical solutions to FGM tubes under internal or external pressure and determine the conditions of the yielding of the assembly. In this thesis, four different cases are investigated:

1. FGM tube with free ends under internal pressure
2. FGM tube with free ends under external pressure
3. FGM tube with fixed ends under internal pressure
4. FGM tube with fixed ends under external pressure

A long tube of inner radius a and outer radius b is considered. The geometry of the assembly is shown in Figure 1.2. The modulus of elasticity and the uniaxial yield limit of the tube material are assumed to vary nonlinearly in the radial direction. Under plane strain assumption and considering small deformations, the analytical expressions of stresses and displacement for the four cases stated above are derived first. Then the yielding of the tubes is examined using von Mises yield criterion. In addition, some numerical results are given in order to clarify the yielding behaviour of the FGM tubes.

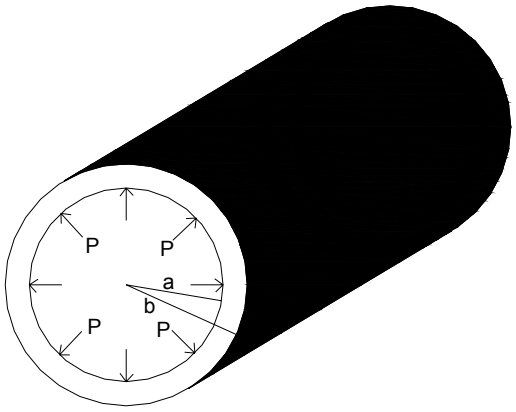

Figure 1.2 General view of the tube assembly

In Chapter II, the analytical expressions for the stresses and displacement are derived for the free and fixed end conditions. Using the boundary conditions (internal or

external pressure) the corresponding integration constants are obtained. In addition to these, von Mises criterion is determined for the pressurized tube assembly for defining the yielding behaviour.

Studies show that the FGM tubes may yield at the inner surface, at the outer surface or simultaneously at both surfaces. The numerical results that clarify this phenomenon are given in Chapter III. Some parametric studies are also performed in this chapter to show the effect of the FGM parameters on the elastic limit pressure. Finally in the last chapter, a brief summary together with a conclusion part is given.

CHAPTER II

FORMULATION AND SOLUTION

2.1 General

Cylindrical polar coordinates (r, θ, z) are used in the derivations. Under plane strain condition and assuming small deformations, the governing differential equations for the FGM tubes with free and fixed ends are derived first. Then, the relations regarding the stresses and displacements for the internal and external pressure cases are obtained. Finally, the yielding behaviour of the FGM tubes due to von Mises yield criterion is presented.

2.2 Solution

The generalized Hooke's law in the radial and circumferential direction is

$$\in_r (r) = \frac{1}{E(r)}(\sigma_r(r) - \nu(\sigma_\theta(r) + \sigma_z(r))\,, \tag{1}$$

$$\in_\theta (r) = \frac{1}{E(r)}(\sigma_\theta(r) - \nu(\sigma_r(r) + \sigma_z(r))\,. \tag{2}$$

The stress component in axial direction can be written as

$$\sigma_z(r) = E(r) \in_z + \nu(\sigma_\theta(r) + \sigma_r(r))\,. \tag{3}$$

If the stress-displacement relations

$$\in_r (r) = \frac{du}{dr}, \tag{4}$$

$$\in_\theta (r) = \frac{u}{r}, \tag{5}$$

and the axial stress expression (Eq.3) is inserted into Eqs. (2) and (3), the following stress-displacement relations are obtained:

$$\sigma_r(r) = \frac{r\nu E(r) \in_z + \nu E(r)u(r) + rE(r)u'(r) - r\nu E(r)u'(r)}{r(1+\nu)(1-2\nu)}, \tag{6}$$

$$\sigma_\theta(r) = \frac{r\nu E(r) \in_z + E(r)u(r) - \nu E(r)u(r) + r\nu E(r)u'(r)}{r(1+\nu)(1-2\nu)}. \tag{7}$$

For the FGM tube, the modulus of elasticity is assumed to be in the form of

$$E(r) = E_0\left(\frac{r}{b}\right)^n. \tag{8}$$

Here E_0 is the reference value of E, r the radial coordinate, b the outer diameter and n is the FGM parameter. The variation of the dimensionless modulus of elasticity (E / E_0) along the radial coordinate is given in Fig. 2.1 for different n values.

Inserting the stress expressions in Eqs. (6) and (7) into the equation of equilibrium

$$\sigma_r + r\,\frac{d\sigma_r}{d_r} - \sigma_\theta(r) = 0 \quad , \tag{9}$$

gives

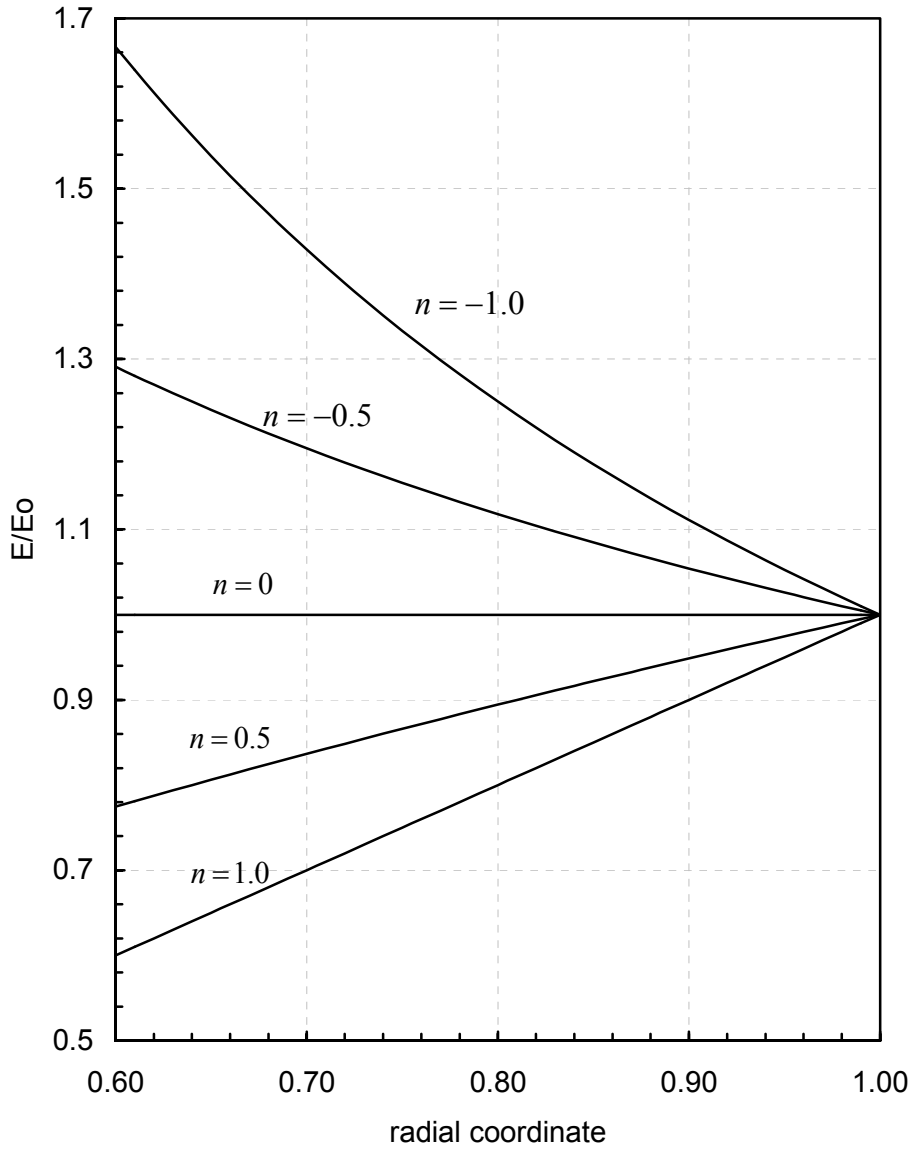

Figure 2.1 The variation of modulus of elasticity along the radial coordinate

$$r^2(-1+\nu)\frac{d^2u}{dr^2}+(1+n)r(-1+\nu)\frac{du}{dr}+(1+(-1-n)\nu)u=nr\nu\in_z. \qquad (10)$$

This is the governing differential equation which has the solution

$$u(r)=C_1\, r^{-(n-K)/2} + C_2 r^{-(n+K)/2} - r\nu \in_z , \tag{11}$$

where C_1 and C_2 are the integration constants and

$$K = \sqrt{\frac{4+n^2-(2+n)^2\nu}{(1-\nu)}} . \tag{12}$$

In the next part, the solutions of the four cases, which are mentioned previously, are presented.

2.3 FGM tubes with free ends

For free ends, a generalized plane strain condition is considered, where $\in_z$ = constant . The corresponding stress expression are obtained as

$$\sigma_r(r) = -\frac{E_0}{2(1+\nu)(1-2\nu)b^n}\begin{bmatrix} C_1 r^{(K+n-2)/2}(n-K(1-\nu)-(2+n)\nu) \\ + C_2 r^{(n-K-2)/2}(K+n-(2+K+n)\nu) \end{bmatrix}, \tag{13}$$

$$\sigma_\theta(r) = \frac{E_0}{2(1+\nu)(1-2\nu)b^n}\begin{bmatrix} C_1 r^{(K+n-2)/2}(2-(2-K+n)\nu) \\ + C_2 r^{(n-K-2)/2}(2-(2+K+n)\nu) \end{bmatrix}, \tag{14}$$

$$\sigma_z(r) = \frac{E_0}{2(1+\nu)(1-2\nu)b^n}\begin{bmatrix} C_1 r^{(K+n-2)/2}(2+K-n)\nu \\ + C_2 r^{(n-K-2)/2}(2-K-n)\nu \end{bmatrix} + \left(\frac{r}{b}\right)^n E_0 \in_z . \tag{15}$$

The displacement relation for free end case is given in Eq. (11).

2.3.1 Free ends-internal pressure

Using the boundary conditions $\sigma_r(a) = -P$ and $\sigma_r(b) = 0$, the integration constants are obtained as

$$C_1 = \frac{2a^{(2+K-n)/2} P(1+\nu)(1-2\nu)}{(a^K - b^K) b^{-n} (n - K(1-\nu) - (2+n)\nu) E_0}, \tag{16}$$

$$C_2 = -\frac{2a^{(2+K-n)/2} P(1+\nu)(1-2\nu)}{(a^K - b^K) b^{-(n+K)} (n + K - (2+K+n)\nu) E_0}. \tag{17}$$

Since the ends of the shafts are free, the net force in axial direction vanishes, that is

$$\int \sigma_z(r) \cdot r \cdot dr = 0. \tag{18}$$

Using this equation, the strain in axial direction is obtained as

$$\in_z = \frac{a^2 (2+n) P \nu}{(a^{2+n} - b^{2+n}) E_0 b^{-n}}. \tag{19}$$

2.3.2 Free ends-external pressure

For the external pressure case, the boundary conditions are $\sigma_r(a) = 0$ and $\sigma_r(b) = -P$. The integration constants are obtained as

$$C_1 = \frac{2b^{(2+K+n)/2} P(1+\nu)(1-2\nu)}{(-a^K + b^K)(n - K(1-\nu) - (2+n)\nu) E_0}, \tag{20}$$

$$C_2 = \frac{2a^K b^{(2+K+n)/2} P(1+\nu)(1-2\nu)}{(a^K - b^K)(K + n - (2+K+n)\nu) E_0}. \tag{21}$$

Using Eq. (18), the axial strain for the external pressure case is found as

$$\in_z = -\frac{b^{2+n}(2+n)P\nu}{(a^{2+n}-b^{2+n})E_0}. \tag{22}$$

2.4 FGM tubes with fixed ends

For fixed ends, the strain in axial direction $\in_z = 0$. The governing differential equation becomes

$$r^2(-1+\nu)\frac{d^2u}{dr^2}+(1+n)r(-1+\nu)\frac{du}{dr}+(1+(-1-n)\nu)u=0. \tag{23}$$

The solution of this equation gives

$$u(r)=C_1\, r^{-(n-K)/2}+C_2 r^{-(n+K)/2}. \tag{24}$$

and the corresponding stress expression are obtained as

$$\sigma_r(r) = -\frac{E_0}{2(1+\nu)(1-2\nu)b^n}\begin{bmatrix} C_1 r^{(K+n-2)/2}(n-K(1-\nu)-(2+n)\nu) \\ +C_2 r^{(n-K-2)/2}(K+n-(2+K+n)\nu)\end{bmatrix}, \tag{25}$$

$$\sigma_\theta(r) = \frac{E_0}{2(1+\nu)(1-2\nu)b^n}\begin{bmatrix} C_1 r^{(K+n-2)/2}(2-(2-K+n)\nu) \\ +C_2 r^{(n-K-2)/2}(2-(2+K+n)\nu)\end{bmatrix}, \tag{26}$$

$$\sigma_z(r) = \frac{E_0}{2(1+\nu)(1-2\nu)b^n}\begin{bmatrix} C_1 r^{(K+n-2)/2}(2+K-n)\nu \\ +C_2 r^{(n-K-2)/2}(2-K-n)\nu\end{bmatrix}, \tag{27}$$

2.4.1 Fixed ends-internal pressure

Using the boundary conditions $\sigma_r(a) = -P$ and $\sigma_r(b) = 0$, the integration constants are obtained as

$$C_1 = \frac{2a^{(2+K-n)/2} P(1+\nu)(1-2\nu)}{(a^K - b^K) b^{-n} (n - K(1-\nu) - (2+n)\nu) E_0}, \tag{28}$$

$$C_2 = -\frac{2a^{(2+K-n)/2} P(1+\nu)(1-2\nu)}{(a^K - b^K) b^{-(n+K)} (n + K - (2+K+n)\nu) E_0}. \tag{29}$$

2.4.2 Fixed ends-external pressure

For the external pressure case, the boundary conditions are $\sigma_r(a) = 0$ and $\sigma_r(b) = -P$. The integration constants are obtained as

$$C_1 = \frac{2b^{(2+K+n)/2} P(1+\nu)(1-2\nu)}{(-a^K + b^K)(n - K(1-\nu) - (2+n)\nu) E_0} \tag{30}$$

$$C_2 = \frac{2a^K b^{(2+K+n)/2} P(1+\nu)(1-2\nu)}{(a^K - b^K)(K + n - (2+K+n)\nu) E_0} \tag{31}$$

In the following part, the yielding behaviour of the FGM tube assemblies is presented.

2.5 Yielding of FGM tubes under pressure

Since the analytical solutions are obtained, the yielding behaviour of the FGM tubes under pressure can be studied. The von Mises yield criterion [24] in a cylindrical coordinate system can be expressed as

$$\sigma_Y = \sqrt{\frac{1}{2}[(\sigma_r - \sigma_\theta)^2 + (\sigma_r - \sigma_z)^2 + (\sigma_\theta - \sigma_z)^2]}, \tag{32}$$

where σ_Y is the von Mises yield stress. For $\sigma_Y = \sigma_0$, yielding starts and for the cases where $\sigma_Y < \sigma_0$ the assembly is in elastic stress state. It is assumed that the uniaxial yield limit of the material is in the form of

$$\sigma_0(r) = \sigma_C \left(\frac{r}{b}\right)^m . \tag{33}$$

Here σ_C is the reference value of the uniaxial yield limit σ_0 and *m* is the FGM parameter. The variation of the dimensionless uniaxial yield limit ($\sigma_0(r)/\sigma_C$) for different *m* values along the radial coordinate is given in Fig. 2.2. Using the graded uniaxial yield limit given in Eq. (33), the von Mises yield criterion at any coordinate r_Y can be written as

$$\sigma_0(r_Y) = \sqrt{\frac{1}{2}[(\sigma_r(r_Y) - \sigma_\theta(r_Y))^2 + (\sigma_r(r_Y) - \sigma_z(r_Y))^2 + (\sigma_\theta(r_Y) - \sigma_z(r_Y))^2]} . \tag{34}$$

Dividing both sides by $\sigma_C \left(\frac{a}{b}\right)^m$ results in

$$\frac{\sigma_0(r_Y)}{\sigma_C \left(\frac{a}{b}\right)^m} = \frac{1}{\sigma_C \left(\frac{a}{b}\right)^m} \sqrt{\frac{1}{2}[(\sigma_r(r_Y) - \sigma_\theta(r_Y))^2 + (\sigma_r(r_Y) - \sigma_z(r_Y))^2 + (\sigma_\theta(r_Y) - \sigma_z(r_Y))^2]} . \tag{35}$$

Introducing the dimensionless stress expression

$$\bar{\sigma}_i = \frac{\sigma_i}{\sigma_0(a)} . \tag{36}$$

the expression in Eq. (35) becomes

$$\phi = \left(\frac{a}{r_Y}\right)^m \sqrt{\frac{1}{2}[(\bar{\sigma}_r(r_Y) - \bar{\sigma}_\theta(r_Y))^2 + (\bar{\sigma}_r(r_Y) - \bar{\sigma}_z(r_Y))^2 + (\bar{\sigma}_\theta(r_Y) - \bar{\sigma}_z(r_Y))^2]} , \tag{37}$$

where ϕ is the non-dimensional stress variable. It should be noted that the yielding occurs as soon as $\phi = 1$ and for $\phi < 1$ the tube is in elastic stress state. Using this equation, the commencement of the yielding of the FGM tubes can be monitored and the corresponding elastic limit pressures (internal or external) can be evaluated.

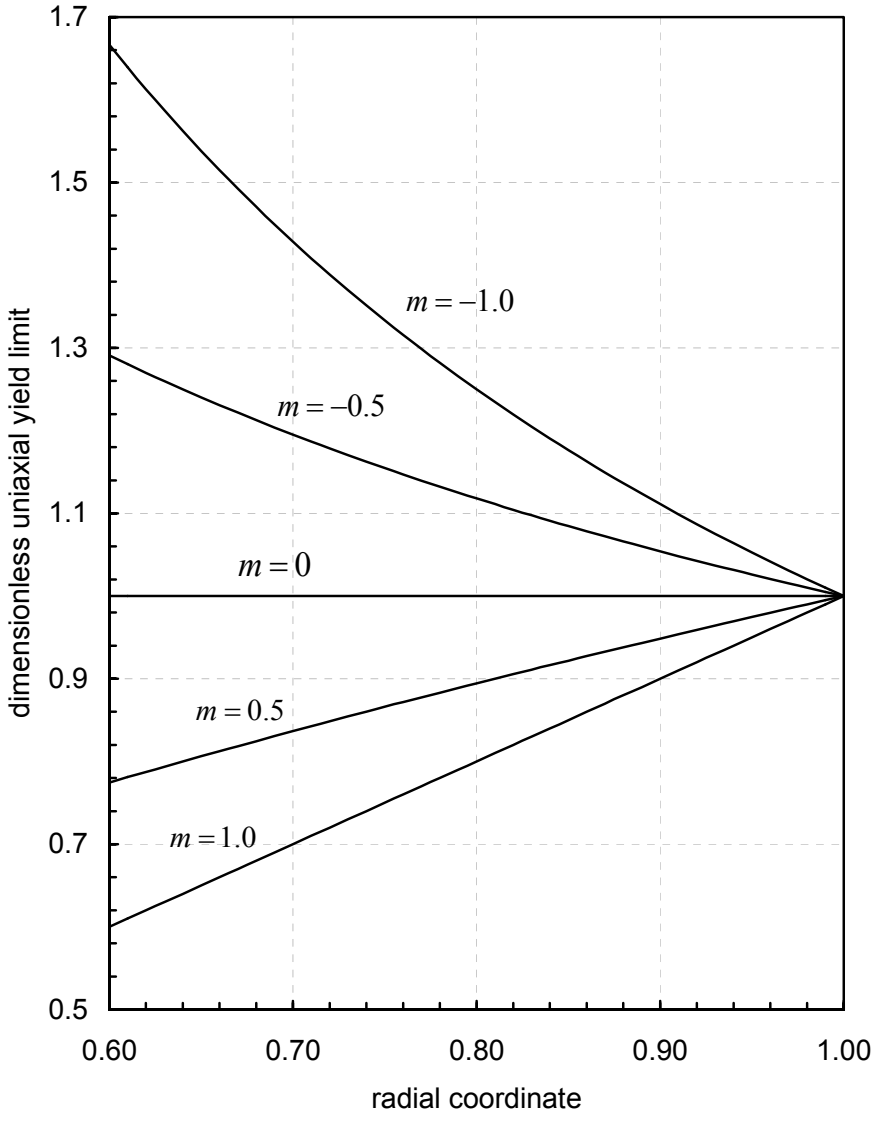

Figure 2.2 The variation of dimensionless uniaxial yield limit ($\sigma_0(r)/\sigma_C$) along the radial coordinate

Studies showed that, for the FGM tubes under internal or external pressure different modes of elastic flow may take place depending on the values of FGM parameters n and m. The yielding may commence at the inner surface of the tube ($r = a$) or at the outer surface of the tube ($r = b$). Different from these two yielding behaviours, the yielding may commence at both surfaces simultaneously.

For the yielding that starts at $r = a$, $\phi = 1$ and the von Mises yield criterion becomes

$$\sqrt{\frac{1}{2}[(\overline{\sigma}_r(a) - \overline{\sigma}_\theta(a))^2 + (\overline{\sigma}_r(a) - \overline{\sigma}_z(a))^2 + (\overline{\sigma}_\theta(a) - \overline{\sigma}_z(a))^2]} = 1. \tag{38}$$

Using this expression, the elastic limit pressure that causes yielding at the inner surface can be evaluated numerically for the given material properties. As an example, an internally pressurized free ended tube ($E_0 = 200GPa$, $\sigma_C = 430MPa$ and $\nu = 0.30$) with $a = 0.7$, $b = 1.0$, $n = 0.0$ and $m = 0.1$ is considered. By the numerical solution of Eq. (38), the elastic limit internal pressure that causes yielding at the inner surface is calculated as $\overline{P}_e = P/\sigma_0(a) = 0.283329$.

Similarly, for the yielding that commences at the outer surface, the criteria is obtained as

$$\left(\frac{a}{b}\right)^m \sqrt{\frac{1}{2}[(\overline{\sigma}_r(b) - \overline{\sigma}_\theta(b))^2 + (\overline{\sigma}_r(b) - \overline{\sigma}_z(b))^2 + (\overline{\sigma}_\theta(b) - \overline{\sigma}_z(b))^2]} = 1. \tag{39}$$

As an example for this type of yielding behaviour, an externally pressurize fixed ended tube ($E_0 = 200GPa$, $\sigma_C = 430MPa$ and $\nu = 0.30$) with $a = 0.4$, $b = 1.0$, $n = 1.3$ and $m = -0.9$ is considered. Upon the numerical solution of Eq. (39), the elastic limit external pressure is evaluated as $\overline{P}_e = 0.418163$.

As mentioned previously, the yielding may begin at both surfaces simultaneously. By the numerical solution of Eqs.(38) and (39) at the same time, one of the FGM parameters (m or n) and the corresponding elastic limit pressure $\overline{P}_e$ that cause yielding at both ends can be evaluated. As an example, a fixed ended tube

($E_0 = 200GPa$, $\sigma_C = 430MPa$ and $\nu = 0.30$) under internal pressure is considered. For $a = 0.65$ and $b = 1.0$, and assigning $n = 1.1205$, the solution of the Eqs. (38) and (39) gives $\overline{P}_e = 0.4$ and $m = -0.944999$. On the other hand, for the same tube for $m = -0.944999$, the numerical solution of the equations results in $n = 1.1205$, and $\overline{P}_e = 0.4$. It may also be possible to evaluate the two FGM parameters m and n that cause yielding at both ends by assigning the elastic limit pressure $\overline{P}_e$. A comprehensive analysis on the yielding behaviour of the FGM tubes is presented in the next chapter.

CHAPTER III

NUMERICAL RESULTS

3.1 General

One of the main purposes of this study is to examine the yielding behaviour of pressurized tubes made of functionally graded materials. The location of the yielding along the tube, the elastic limit pressure that causes plastic flow and the critical FGM parameters are the research interests of this investigation. In this chapter, a comprehensive stress analysis is performed on four different cases: (1) Free ends-internal pressure, (2) free ends-external pressure, (3) fixed ends-internal pressure, and (4) fixed ends-external pressure. For the presentation of the numerical results, the following formal dimensionless variables are used:

$$\bar{r} = \frac{r}{b} \;;\; \bar{\sigma}_i = \frac{\sigma_i}{\sigma_0(a)} \;;\; \bar{u} = \frac{uE_0}{\sigma_0(a)b} \;;\; \overline{C}_1 = \frac{C_1}{b^{(2-n+K)/2}} \;;\; \overline{C}_2 = \frac{C_2}{b^{(2-n-K)/2}} \qquad (40)$$

In the analyses, the mechanical properties of steel are used in all cases with the following data:

- Reference value of modulus of elasticity: $E_0 = 200GPa$
- Reference value of uniaxial yield limit: $\sigma_C = 430MPa$
- Poisson's ratio: $\nu = 0.30$

3.2 Yielding of free ended FGM tubes under internal pressure

For the inner radius $\bar{a} = 0.7$ and functionally grading parameters $n = 0.0$ and $m = 0.1$, yielding begins at the inner surface. The elastic limit internal pressure is

obtained as $\overline{P}_e = 0.283329$ by the numerical solution of Eq. (38). The corresponding integration constants are evaluated as $\overline{C}_1 = 2.93676 \times 10^{-4}$ and $\overline{C}_2 = 7.34190 \times 10^{-4}$ and the strain in axial direction is computed as $\in_z = -3.38857 \times 10^{-4}$. The consequent stresses and displacement are given in Fig. 3.1. It should be noted that the stress variable $\phi = 1$ at the inner surface.

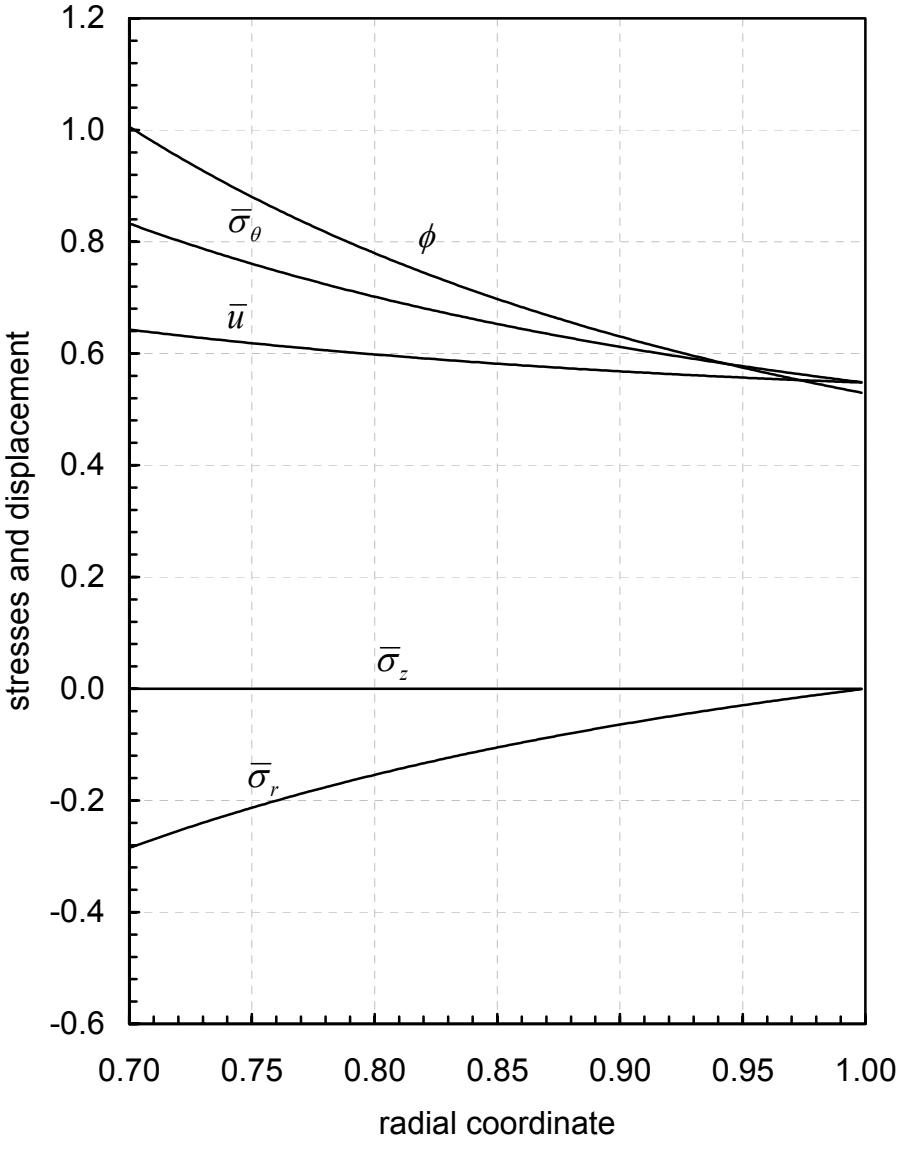

Figure 3.1. The distributions of stresses and displacement in an FGM tube ($\overline{a} = 0.7$, $n = 0.0$ and $m = 0.1$) under internal pressure of $\overline{P}_e = 0.283329$

For the same tube ($\overline{a} = 0.7$), the yielding begins at the outer surface for the material parameters $n = 1.3$ and $m = -0.9$. The corresponding elastic limit internal pressure is evaluated as $\overline{P}_e = 0.300248$ using Eq. (39) and the integration constants are calculated as $\overline{C}_1 = 1.2180 \times 10^{-3}$ and $\overline{C}_2 = 7.49636 \times 10^{-3}$. On the other hand, the strain in the axial direction is calculated as $\in_z = -6.23989 \times 10^{-4}$ using Eq. (19). Fig. 3.2 shows the corresponding distributions of the stresses and displacement.

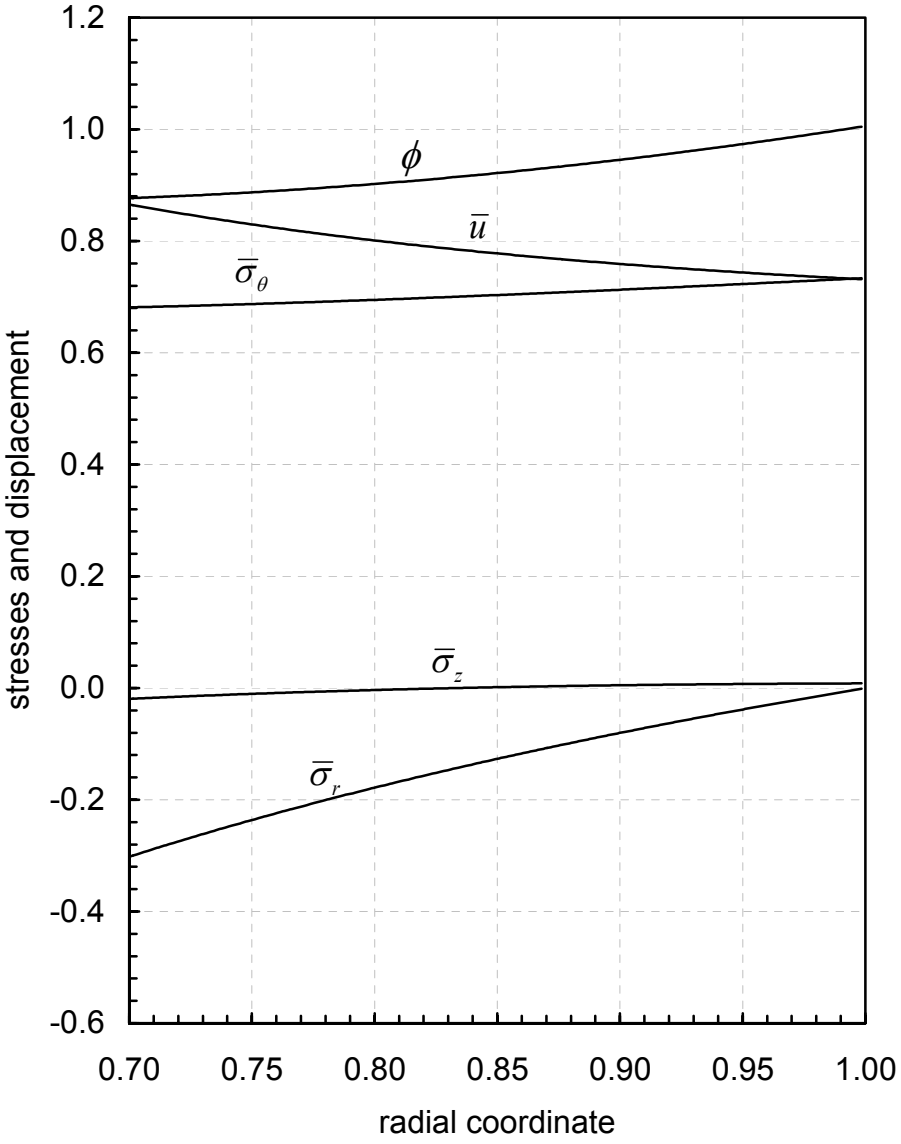

Figure 3.2. The distributions of stresses and displacement in an FGM tube ($\overline{a} = 0.7$, $n = 1.3$ and $m = -0.9$) under internal pressure of $\overline{P}_e = 0.300248$

Finally, for the same tube dimensions, setting $\overline{P}_e = 0.4$ gives the critical FGM parameters $n = 2.27042$ and $m = 0.351816$ by the solution of the Eqs. (38) and (39). The corresponding integration constants and axial strain are obtained as $\overline{C}_1 = 1.59623 \times 10^{-3}$, $\overline{C}_2 = 3.79225 \times 10^{-4}$ and $\in_z = -6.0897 \times 10^{-4}$, respectively. The consequent stresses and displacement is shown in Fig. 3.3. It is observed in this graph that the yielding begins simultaneously at both surfaces since $\phi = 1$ at these locations.

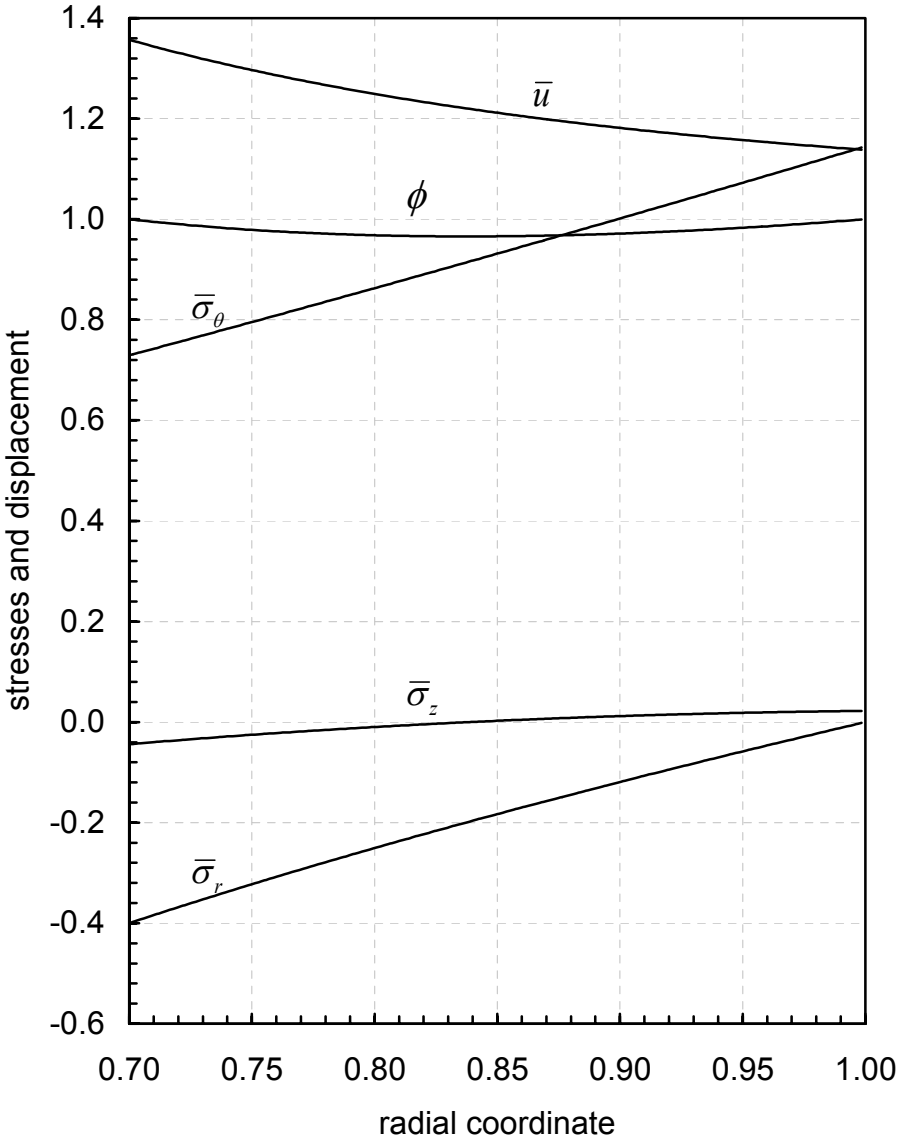

Figure 3.3. The distributions of stresses and displacement in an FGM tube ($\overline{a} = 0.7$, $n = 2.27042$ and $m = 0.351816$) under internal pressure of $\overline{P}_e = 0.4$

3.3 Yielding of free ended FGM tubes under external pressure

For the tube assembly with inner radius $\bar{a} = 0.5$ and functionally grading parameters $n = 0.3$ and $m = 0.3$, yielding begins at the inner surface. The elastic limit external pressure is obtained as $\overline{P}_e = 0.414685$ using Eq. (38). The corresponding integration constants are evaluated as $\overline{C}_1 = -6.01742 \times 10^{-4}$, $\overline{C}_2 = -2.97790 \times 10^{-3}$ and the strain in axial direction is computed as $\in_z = 6.27008 \times 10^{-4}$. The consequent stresses and displacement are given in Fig. 3.4. As seen in this figure, the plastic flow starts at the inner surface since $\phi = 1$ at that location.

For the same tube assembly ($\bar{a} = 0.5$), the yielding begins at the outer surface for the material parameters $n = 1.3$, $m = -0.9$. Using Eq. (39), the corresponding elastic limit external pressure is evaluated as $\overline{P}_e = 0.257289$. The integration constants are calculated as $\overline{C}_1 = -1.49296 \times 10^{-3}$, $\overline{C}_2 = -2.53041 \times 10^{-4}$. and the strain in the axial direction is obtained as $\in_z = 1.13742 \times 10^{-3}$. Fig. 3.5 shows the corresponding distributions of the stresses and displacement.

For $\bar{a} = 0.5$, setting $\overline{P}_e = 0.4$ gives the critical FGM parameters $n = 0.193576$, $m = -0.703840$ by the solution of the Eqs. (38) and (39). The corresponding integration constants and axial strain are obtained as $\overline{C}_1 = -1.0914 \times 10^{-3}$, $\overline{C}_2 = -5.89789 \times 10^{-4}$ and $\in_z = 1.17973 \times 10^{-3}$, respectively. The consequent stresses and displacement is shown in Fig. 3.6. As seen in this figure, at both surfaces $\phi = 1$.

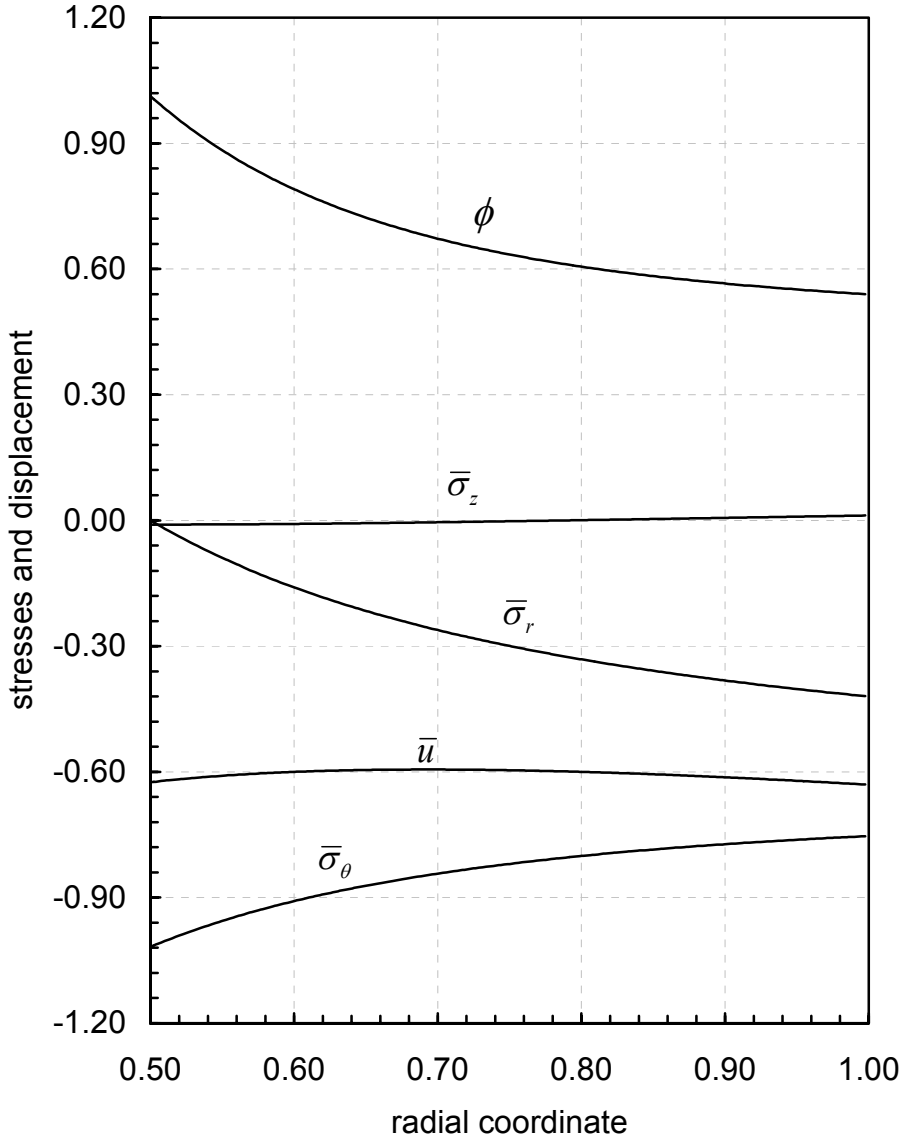

Figure 3.4. The distributions of stresses and displacement in an FGM tube ($\overline{a} = 0.5, n = 0.3$ and $m = 0.3$) under external pressure of $\overline{P}_e = 0.414685$

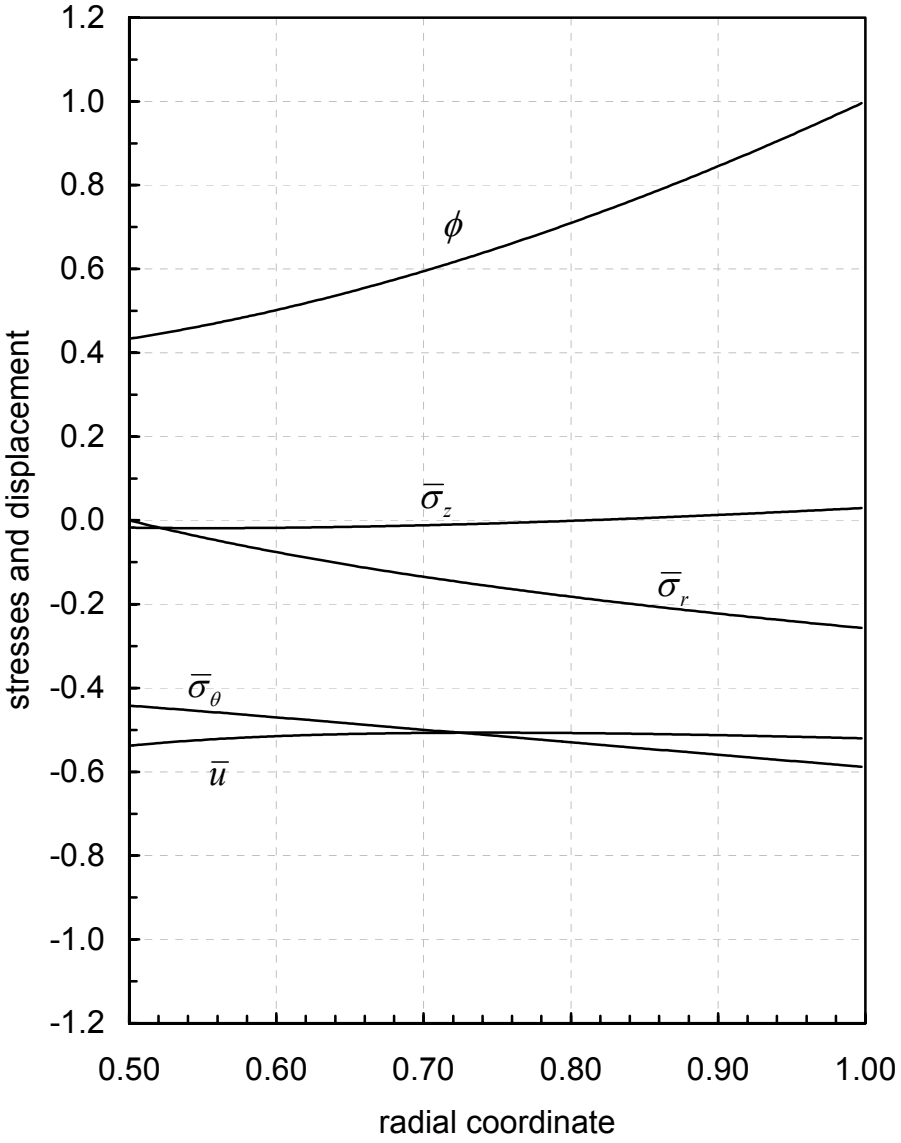

Figure 3.5. The distributions of stresses and displacement in an FGM tube ($\overline{a} = 0.5, n = 1.3$ and $m = -0.9$) under external pressure of $\overline{P}_e = 0.257289$

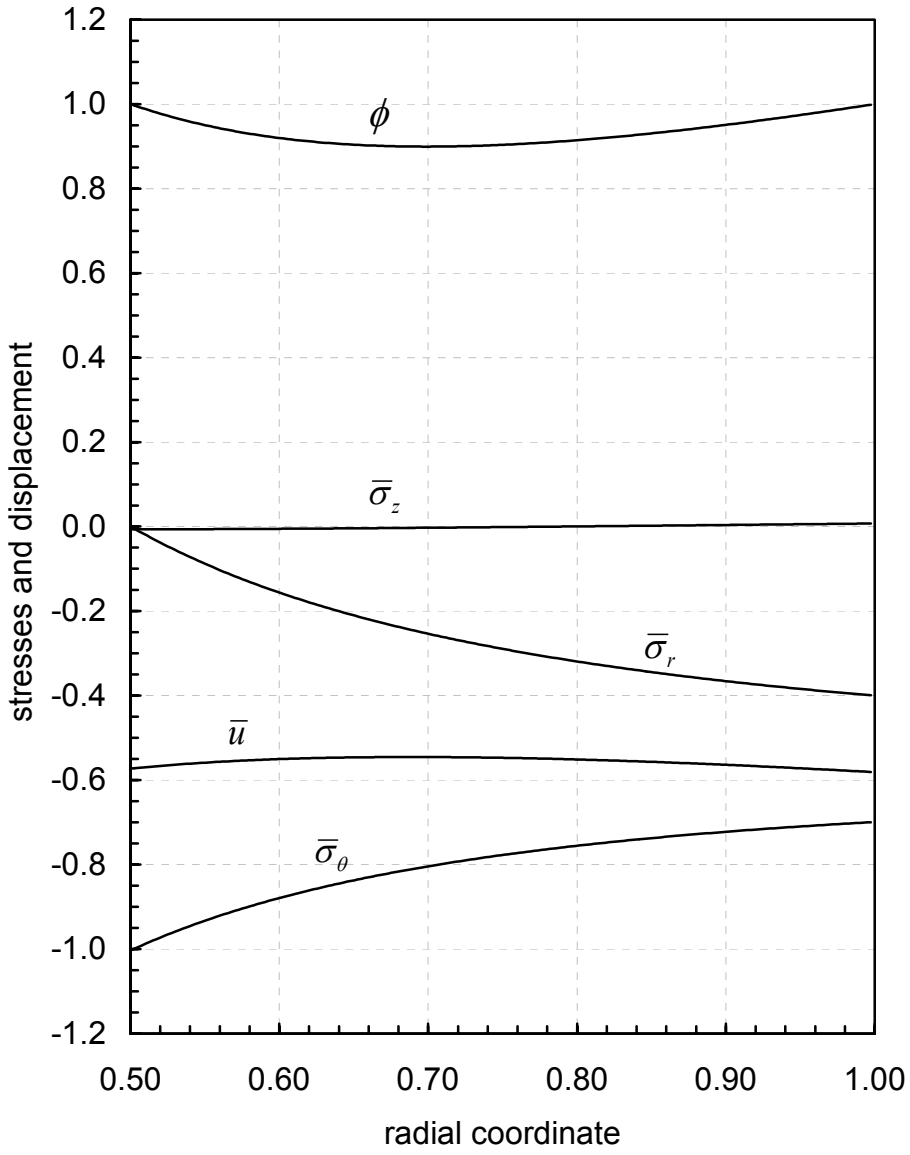

Figure 3.6. The distributions of stresses and displacement in an FGM tube ($\overline{a} = 0.5, n = 0.193576$ and $m = -0.703840$) under external pressure of $\overline{P}_e = 0.4$

3.4 Yielding of fixed ended FGM tubes under internal pressure

For the tube assembly with inner radius $\overline{a} = 0.65$ and functionally grading parameters $n = 0.3$ and $m = 0.1$, yielding begins at the inner surface. The elastic

limit internal pressure is obtained as $\overline{P}_e = 0.348650$ using Eq. (38) and the corresponding integration constants are evaluated as $\overline{C}_1 = 3.60845 \times 10^{-4}$, $\overline{C}_2 = 6.62299 \times 10^{-4}$. The consequent stresses and displacement are given in Fig. 3.7. The plastic flow starts at the inner surface since $\phi = 1$ at that location.

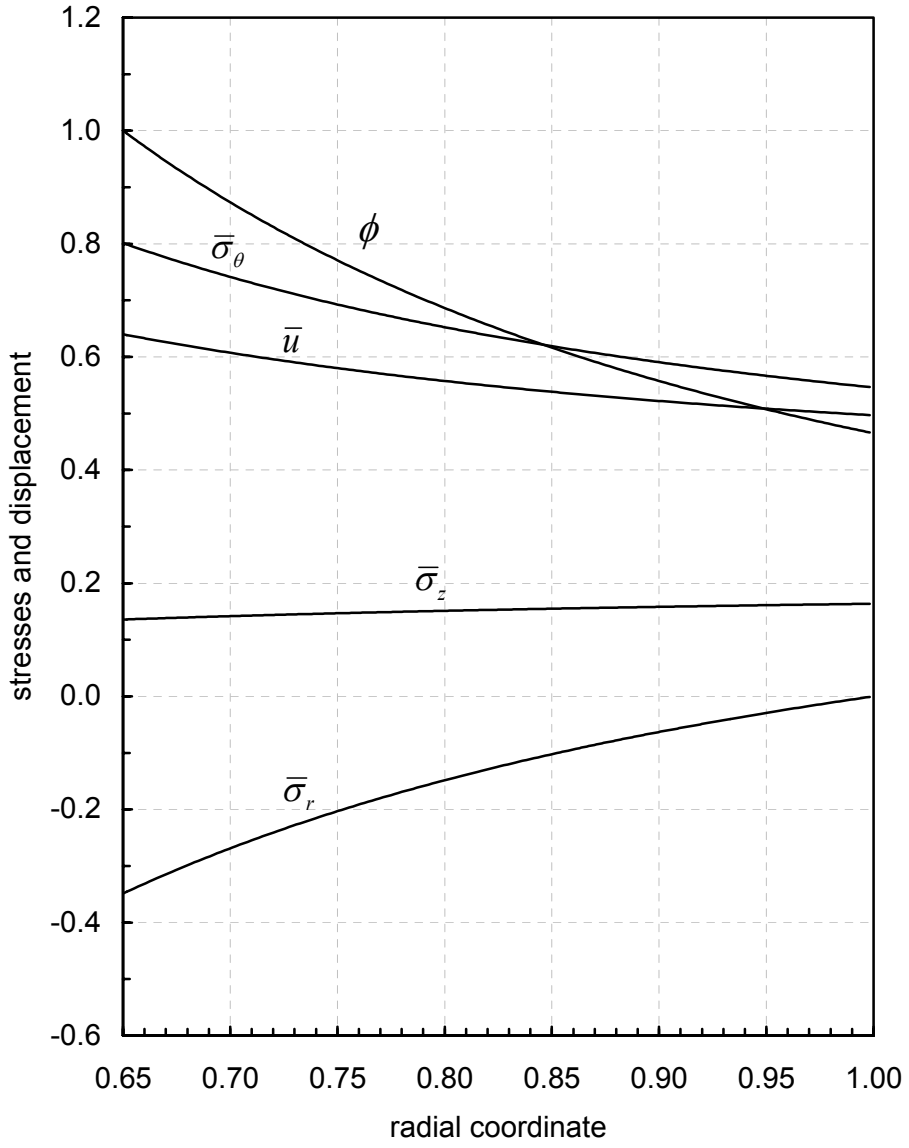

Figure 3.7. The distributions of stresses and displacement in an FGM tube ($\overline{a} = 0.65, n = 0.3$ and $m = 0.1$) under internal pressure of $\overline{P}_e = 0.348650$

For the tube assembly with the same geometry, taking $n = 1.3$ and $m = -0.9$ causes yielding at the outer surface. The elastic limit internal pressure is obtained as $\overline{P}_e = 0.392744$ (using Eq. (39)) and the corresponding integration constants are evaluated as $\overline{C}_1 = 1.3626 \times 10^{-3}$, $\overline{C}_2 = 8.38635 \times 10^{-4}$. The consequent stresses and displacement are given in Fig. 3.8.

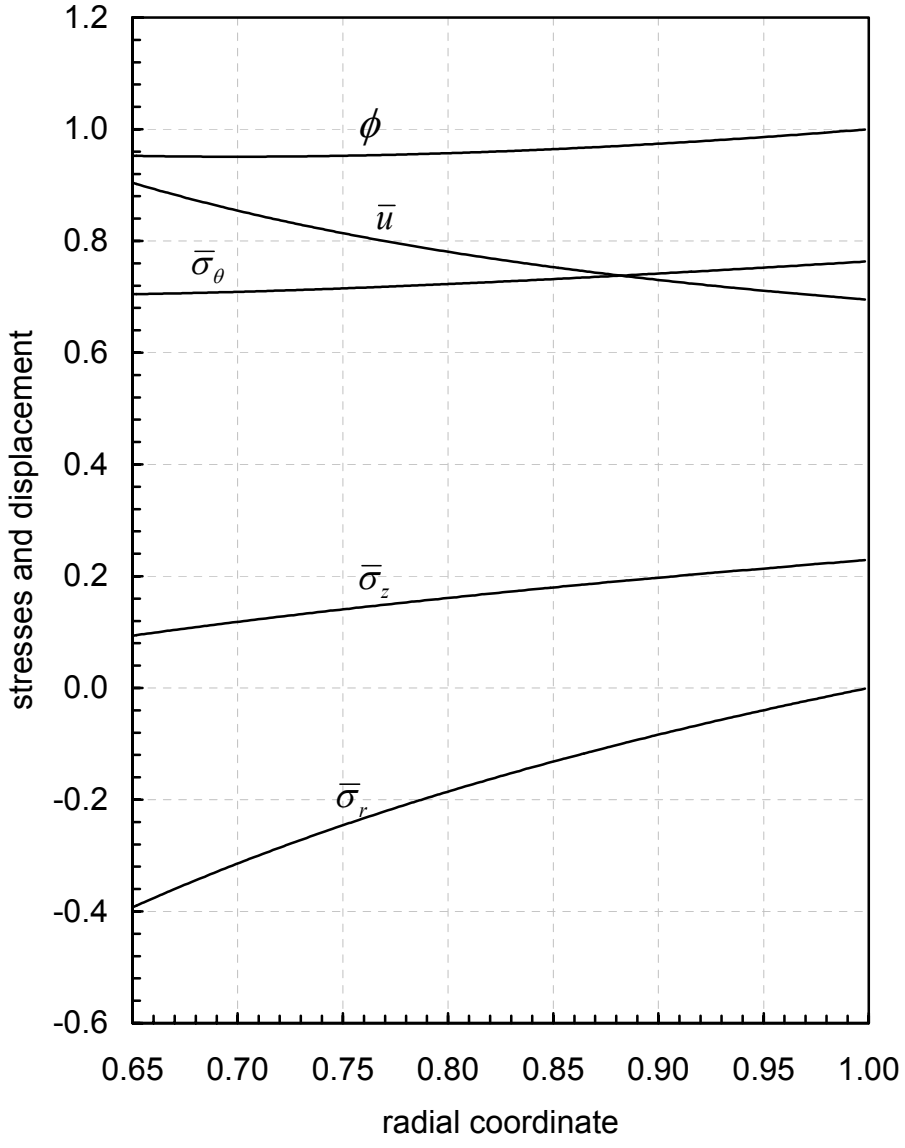

Figure 3.8. The distributions of stresses and displacement in an FGM tube ($\overline{a} = 0.65, n = 1.3$ and $m = -0.9$) under internal pressure of $\overline{P}_e = 0.392744$

Setting $\overline{P}_e = 0.4$ gives the critical FGM parameters $n = 1.1205$, $m = -0.944999$ by the numerical solution of the Eqs. (38) and (39). The corresponding integration constants are obtained as $\overline{C}_1 = 1.25935 \times 10^{-3}$, $\overline{C}_2 = 9.41886 \times 10^{-4}$. The consequent stresses and displacement is shown in Fig. 3.9. As seen in this figure, at both surfaces $\phi = 1$.

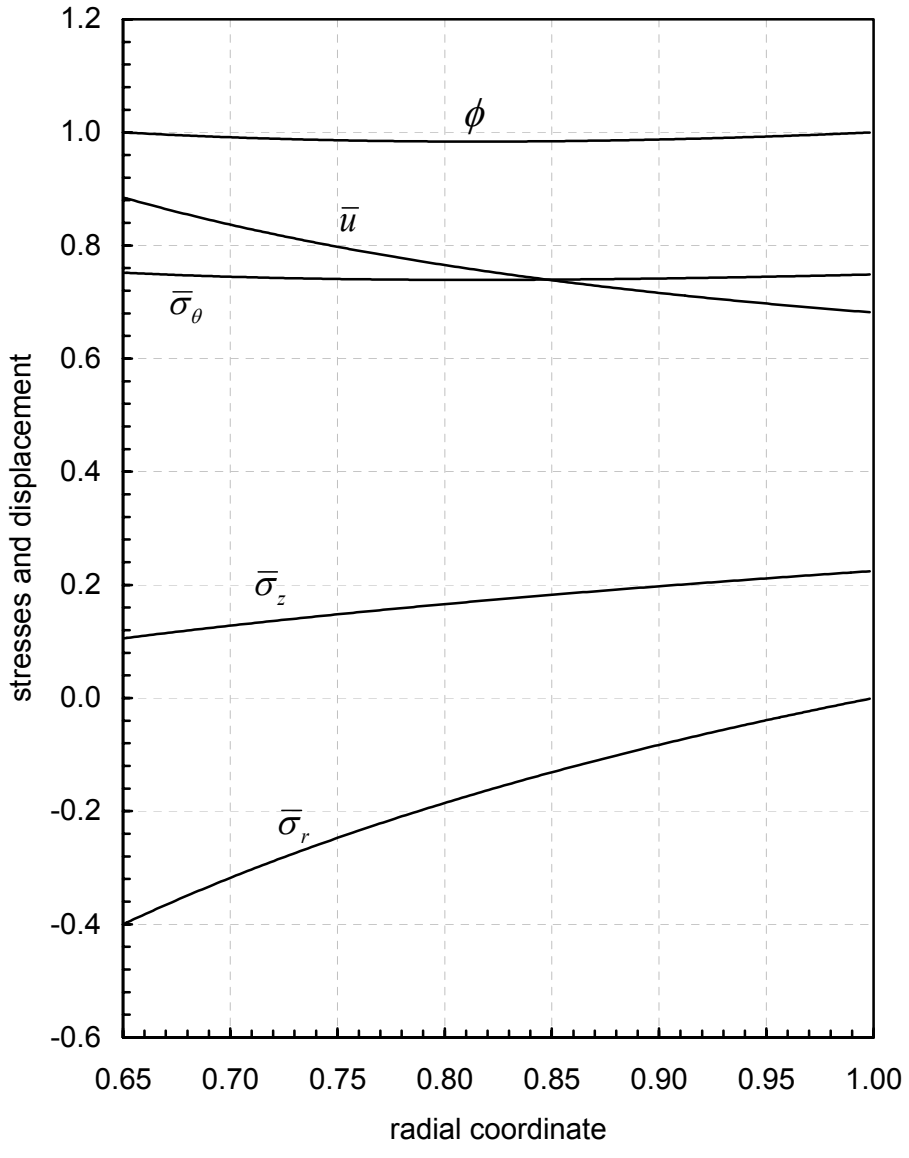

Figure 3.9. The distributions of stresses and displacement in an FGM tube ($\overline{a} = 0.65, n = 1.1205, m = -0.944999$) under internal pressure of $\overline{P}_e = 0.4$

3.5 Yielding of fixed ended FGM tubes under external pressure

For the tube assembly with inner radius $\bar{a} = 0.4$ and functionally grading parameters $n = 0.3$ and $m = 0.1$, yielding begins at the inner surface. Using Eq. (38), the elastic limit external pressure is obtained as $\bar{P}_e = 0.534562$. The corresponding integration constants are evaluated as $\bar{C}_1 = -7.73126 \times 10^{-4}$, $\bar{C}_2 = -2.50898 \times 10^{-4}$. The consequent stresses and displacement are given in Fig. 3.10. The plastic flow starts at the inner surface since $\phi = 1$ at that location.

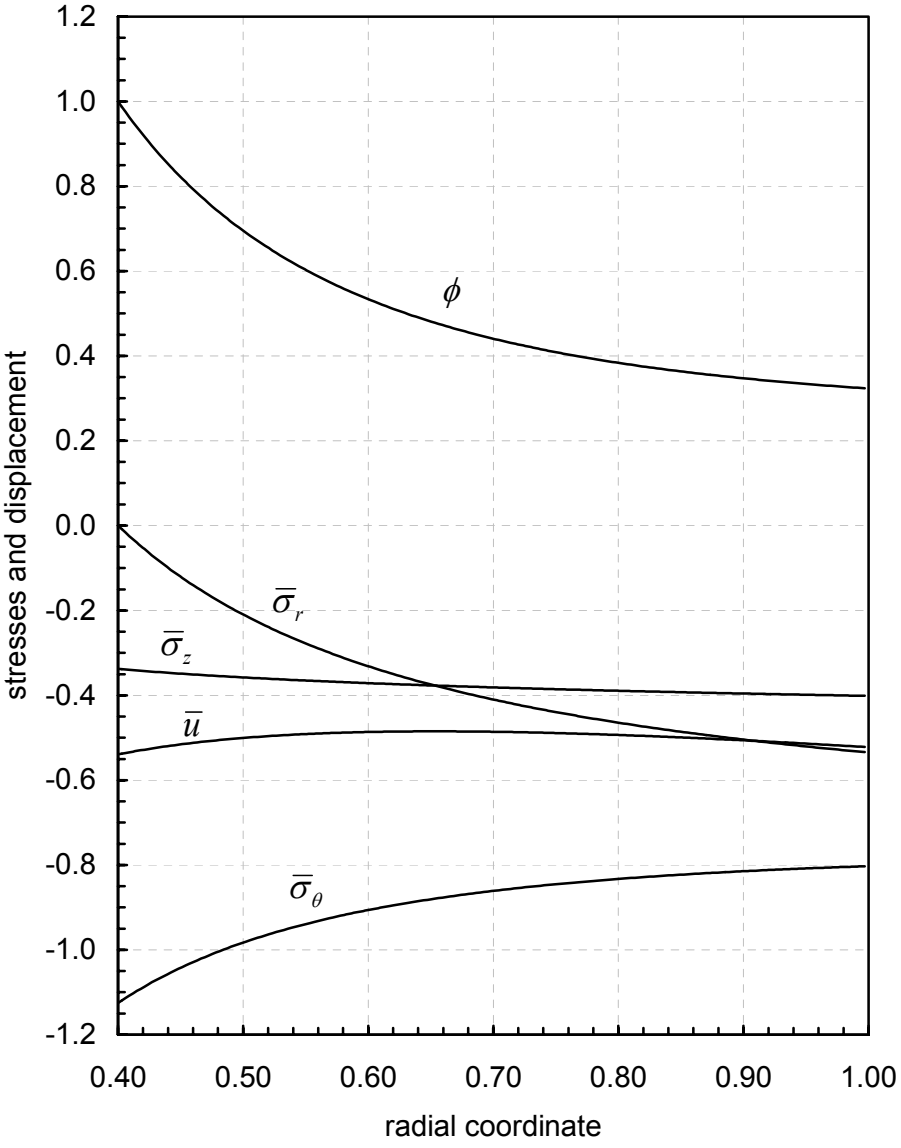

Figure 3.10. The distributions of stresses and displacement in an FGM tube ($\bar{a} = 0.4$, $n = 0.3$ and $m = 0.1$) under external pressure of $\bar{P}_e = 0.534562$

For the tube assembly with inner radius $\overline{a} = 0.4$ and functionally grading parameters $n = 1.3$ and $m = -0.9$, yielding begins at the outer surface. The elastic limit external pressure is obtained as $\overline{P}_e = 0.418163$ and the corresponding integration constants are evaluated as $\overline{C}_1 = -2.62695 \times 10^{-3}$ and $\overline{C}_2 = -2.93963 \times 10^{-4}$. The consequent stresses and displacement are given in Fig. 3.11.

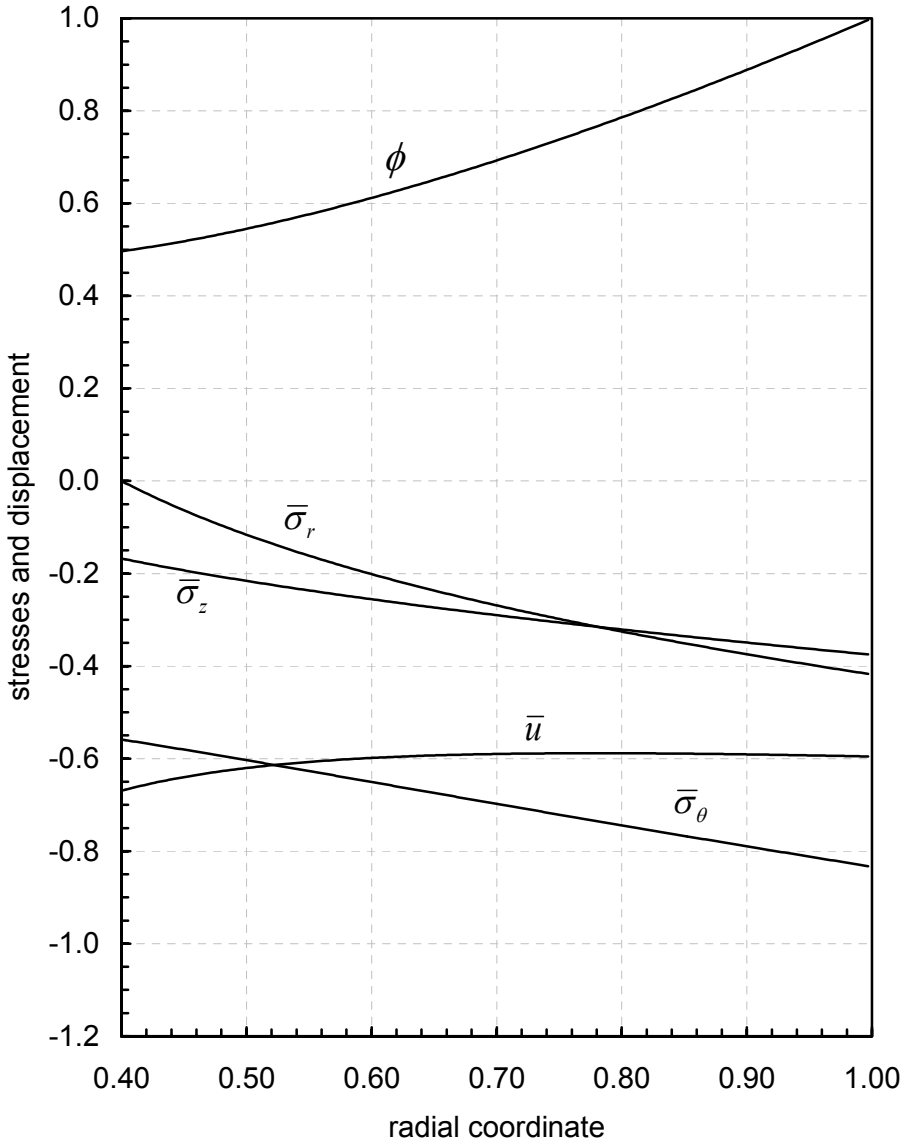

Figure 3.11. The distributions of stresses and displacement in an FGM tube ($\overline{a} = 0.4$, $n = 1.3$ and $m = -0.9$) under external pressure of $\overline{P}_e = 0.418163$

Finally, for the same tube dimensions, setting $\overline{P}_e = 0.4$ gives the critical FGM parameters $n = -0.430149$ and $m = -1.78367$ by the numerical solution of the Eqs. (38) and (39). The corresponding integration constants are obtained as $\overline{C}_1 = -2.14971 \times 10^{-3}$ and $\overline{C}_2 = -1.05968 \times 10^{-3}$. The consequent stresses and displacement is shown in Fig. 3.12. It is observed in this graph that the yielding begins simultaneously at both surfaces since $\phi = 1$ at these locations.

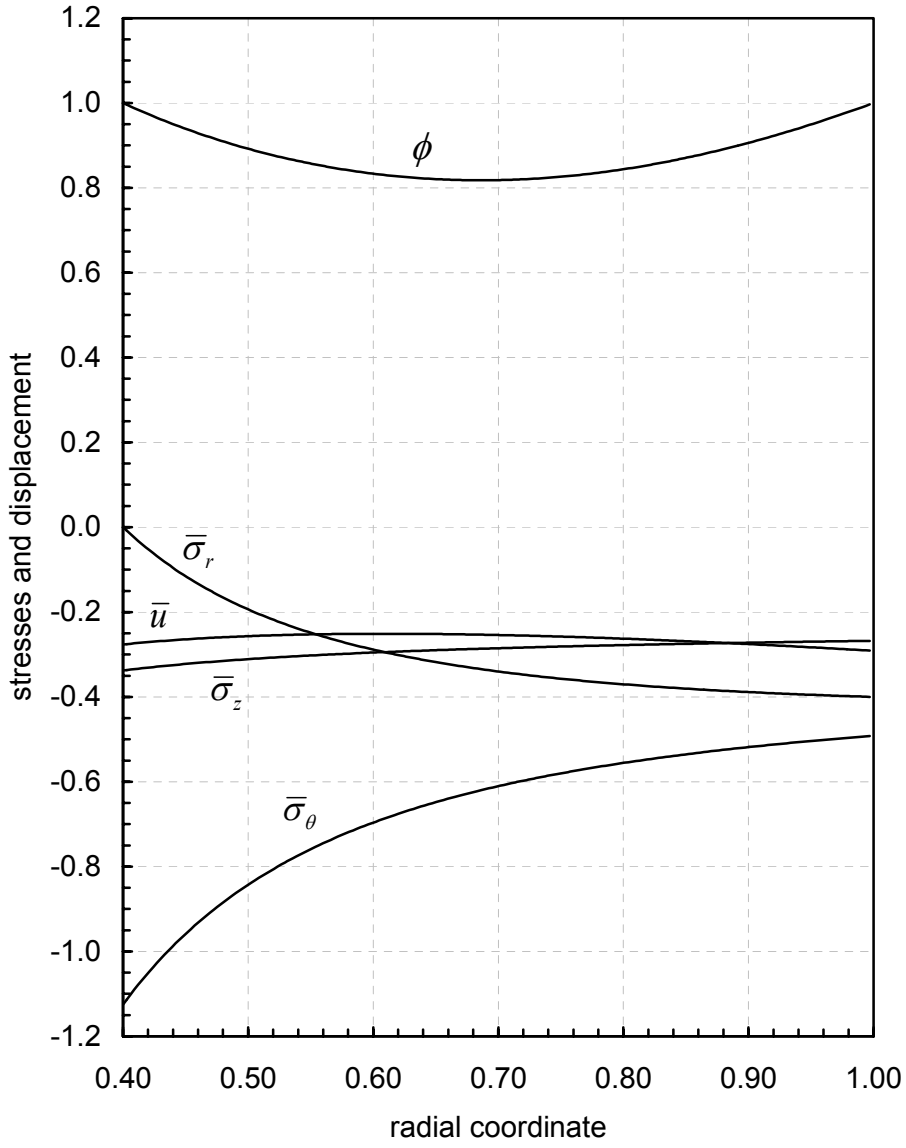

Figure 3.12. The distributions of stresses and displacement in an FGM tube ($\overline{a} = 0.4$, $n = -0.430149$ and $m = -1.78367$) under external pressure of $\overline{P}_e = 0.4$

3.6 Parametric studies

In order to investigate the effect of FGM parameters and inner radius values on the deformation behaviour of the tube assemblies, a number of parametric analyses are performed. To show the effect of the parameter m on the nondimensional stress variable ϕ, an FGM tube with free ends ($\overline{a} = 0.70$ and $n = 2.27042$) under internal pressure is considered. In Fig. 3.13 the variation of the yield variable with different values of m are plotted for the elastic limit internal pressure values. The homogenous case ($m = 0.0,\ n = 0.0$) is also included in this graph.

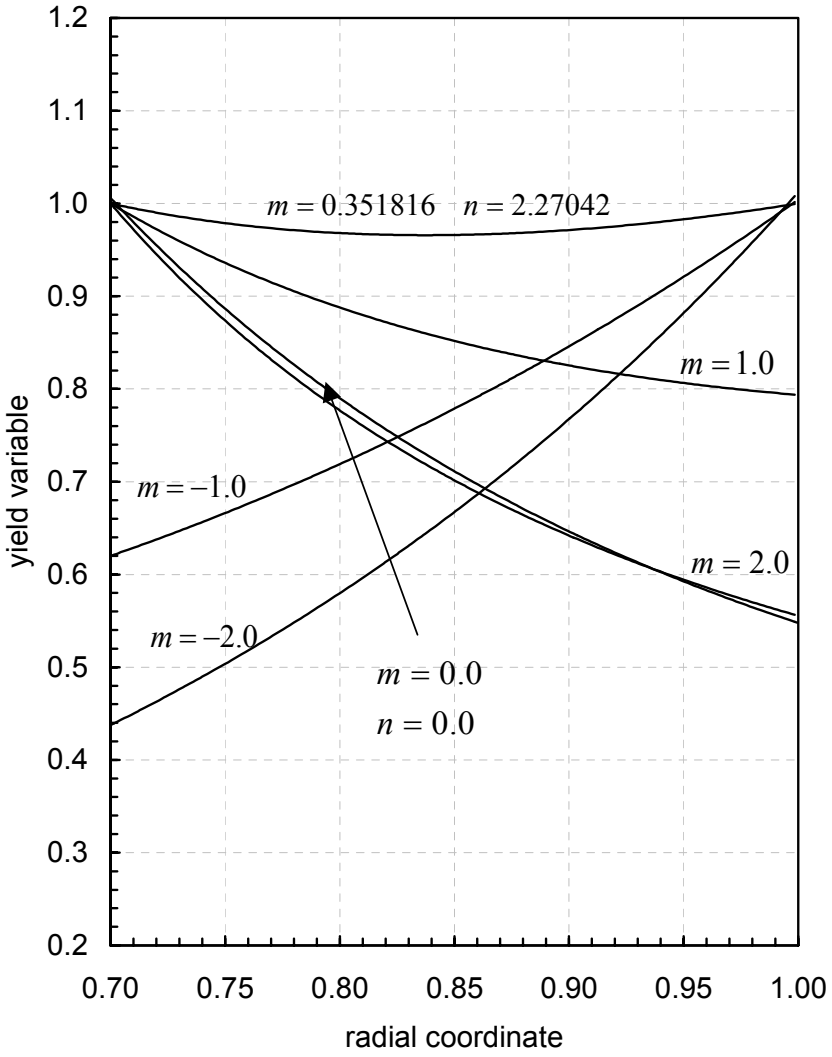

Figure 3.13 Variation of yield variable in free ended FGM tubes under internal pressure for $\overline{a} = 0.70$ and $n = 2.27042$ using m as a parameter

It can be seen in this figure that the location of the yielding changes as the value of the FGM parameter *m* changes. For example, the yielding begins at the inner surface when $m = 1$, while it begins at the outer surface when $m = -1$. On the other hand, Fig.3.14 shows the variation of the elastic limit internal pressure with the inner radius a for different m and n values. In the figure the curve with $m = 0$ and $n = 0$ corresponds to homogenous tube.

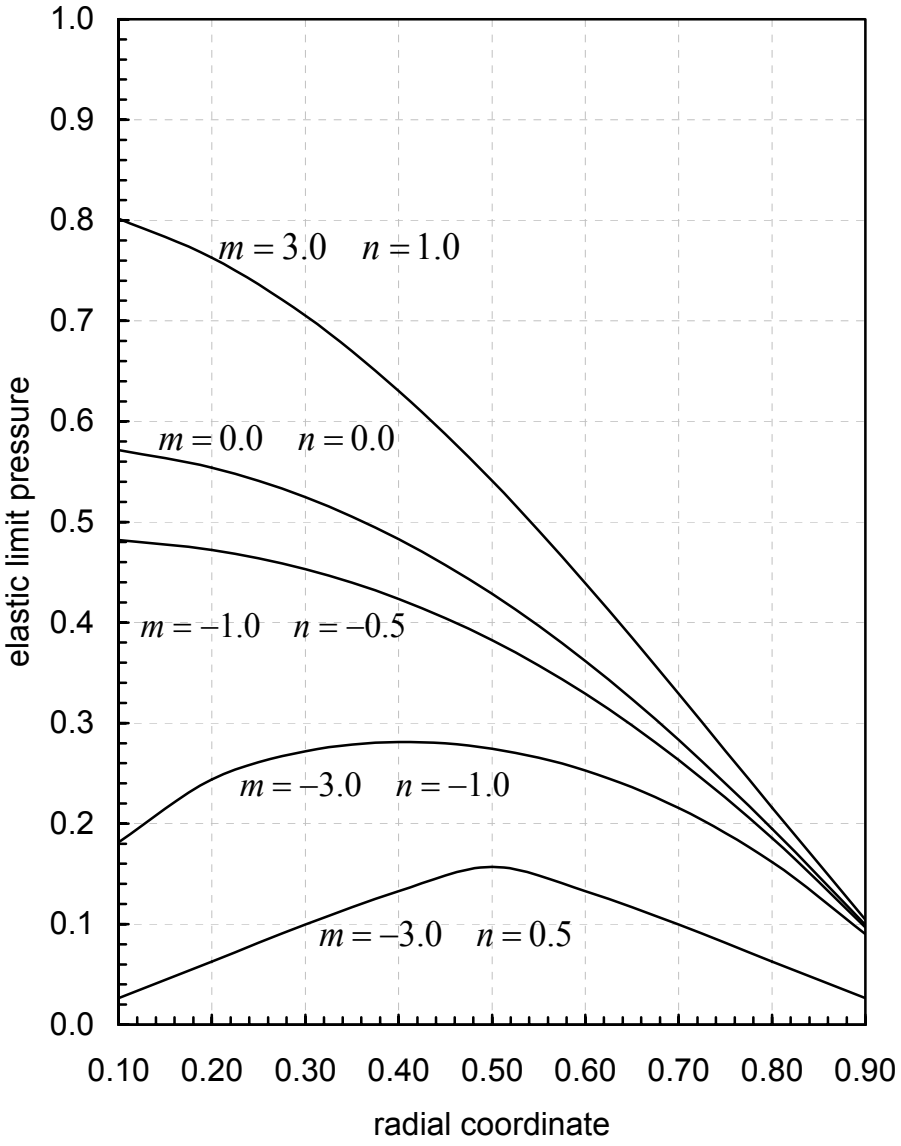

Figure 3.14 Variation of elastic limit internal pressure $\overline{P}_e$ with inner radius a using *n* and *m* as parameters for the FGM tube with free ends

The effect of the parameter m on the nondimensional stress variable ϕ for an FGM tube with free ends ($\overline{a} = 0.50$ and $n = 0.193576$) under external pressure is shown in Fig. 3.15, where the variation of the yield variable with different values of m are plotted for the elastic limit external pressure values. The homogenous case ($m = 0.0,\ n = 0.0$) is also included in this graph.

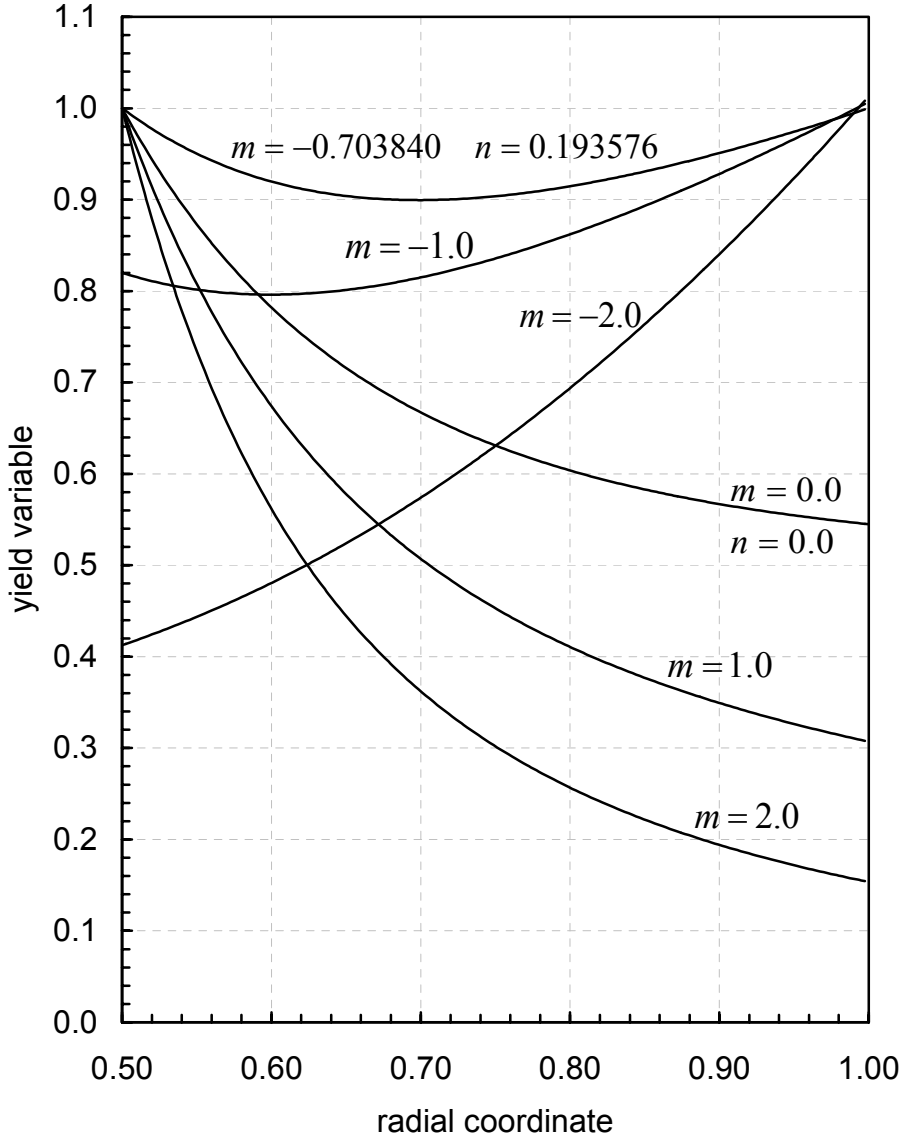

Figure 3.15 Variation of yield variable in free ended FGM tubes under external pressure for $\overline{a} = 0.50$ and $n = 0.193576$ using m as a parameter

Fig. 3.16 shows the variation of the elastic limit external pressure with the inner radius a for different m and n values for an FGM tube with free ends.

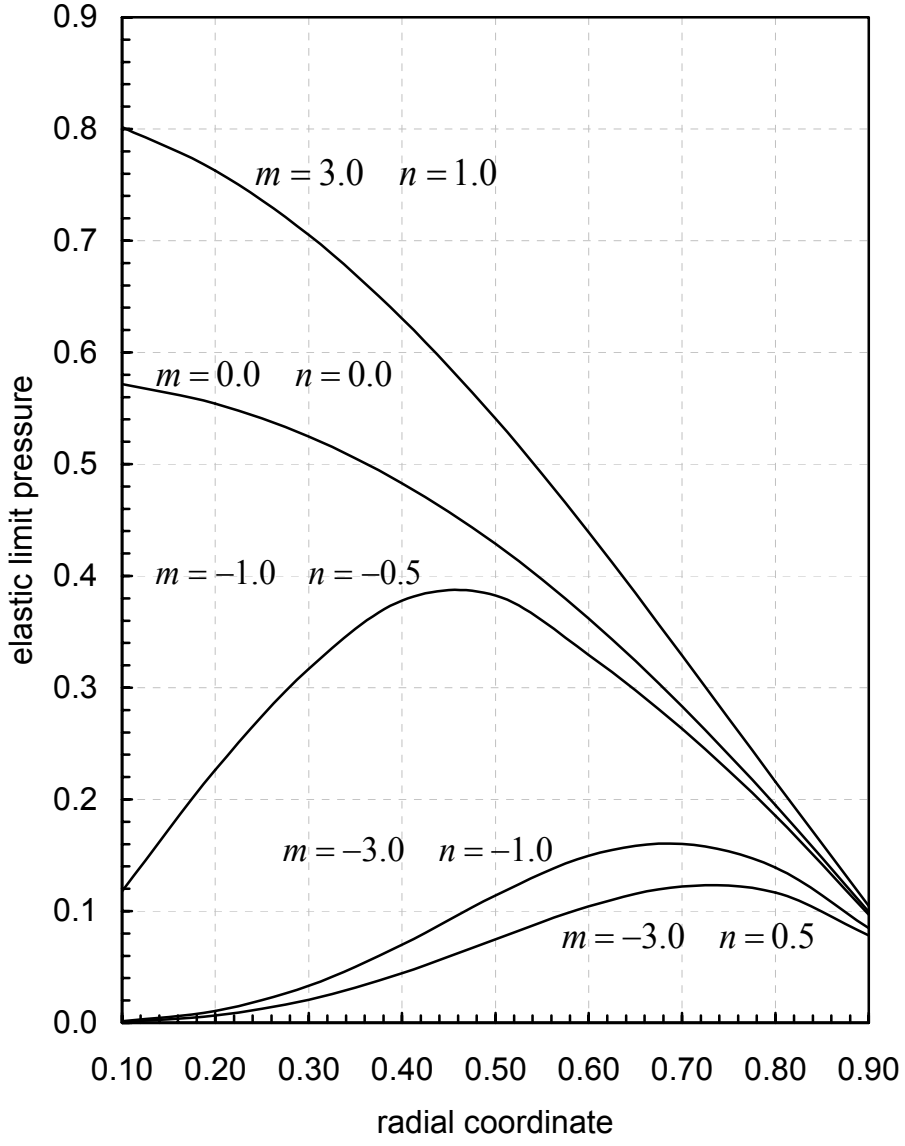

Figure 3.16 Variation of elastic limit external pressure $\overline{P}_e$ with inner radius a using n and m as parameters for the FGM tube with free ends

In order to examine the behaviour of the FGM tubes with fixed ends, a tube assembly (with $\bar{a} = 0.65$ and $n = 1.1205$) under internal pressure is considered. In Fig. 3.17 the variation of the yield variable with different values of m are plotted for the elastic limit internal pressure values.

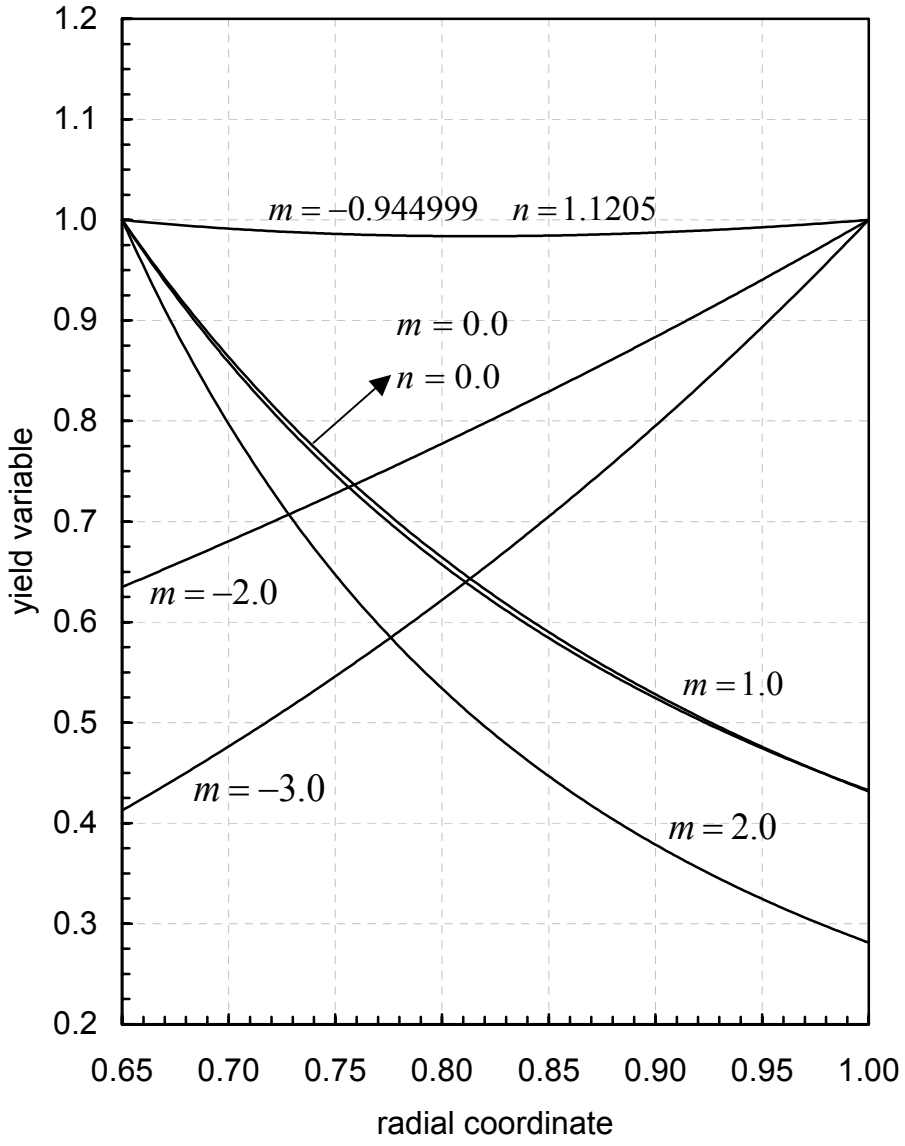

Figure 3.17 Variation of yield variable in fixed ended FGM tubes under internal pressure for $\bar{a} = 0.65$ and $n = 1.1205$ using m as a parameter

On the other hand, Fig.3.18 shows the variation of the elastic limit internal pressure with the inner radius a for different m and n values for an FGM tube with fixed ends.

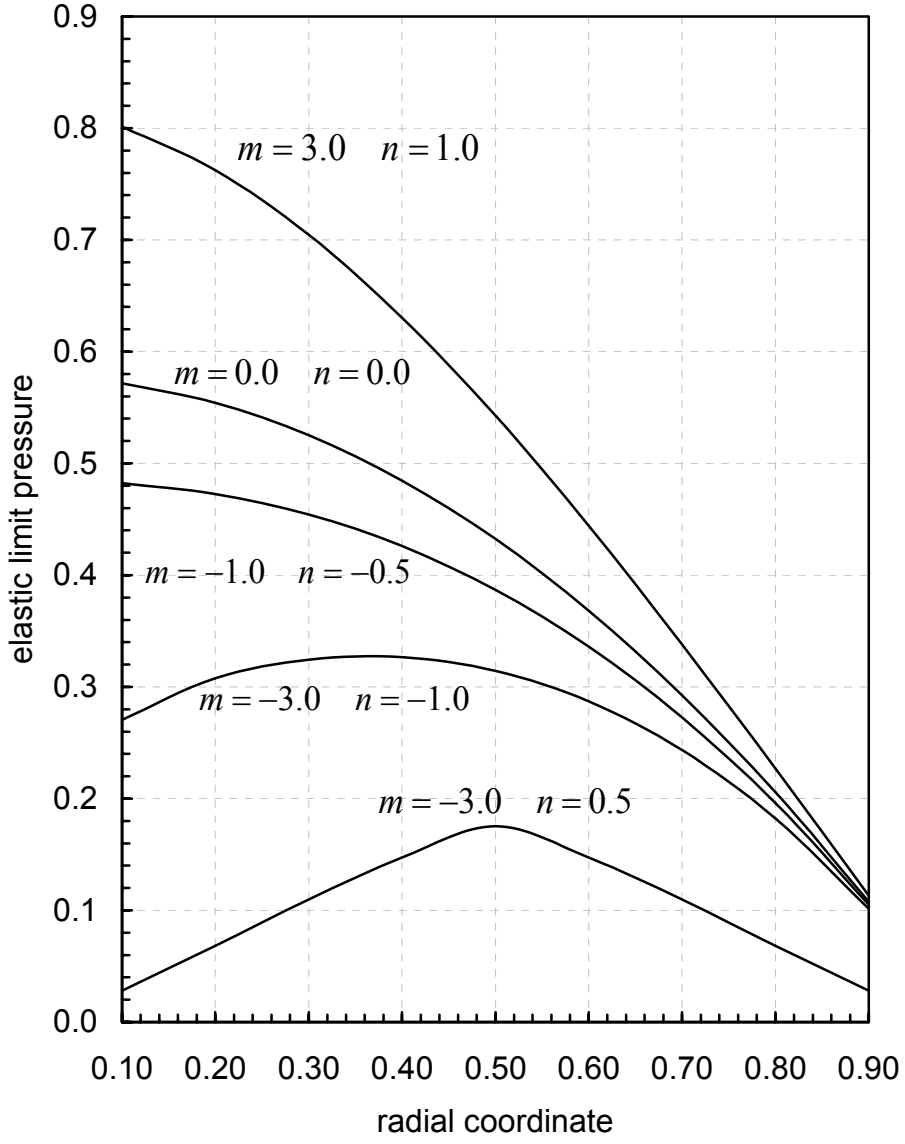

Figure 3.18 Variation of elastic limit internal pressure $\overline{P}_e$ with inner radius a using n and m as parameters for the FGM tube with fixed ends

Finally, for the externally pressurized FGM tubes with fixed ends, an assembly with $\overline{a} = 0.4$ and $n = -0.430149$ is considered. In Fig. 3.19 the variation of the yield variable with different values of m are plotted for the elastic limit external pressure values. The homogenous case is also included.

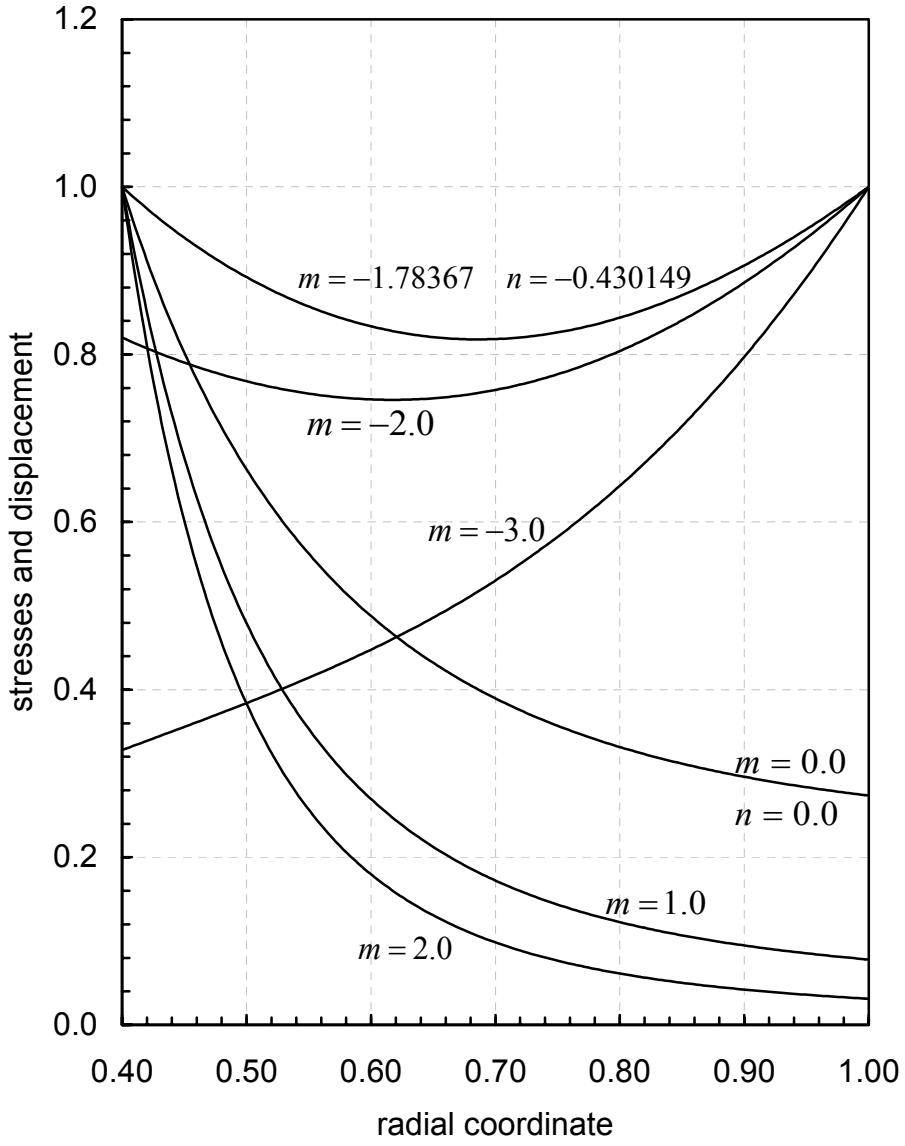

Figure 3.19 Variation of yield variable in fixed ended FGM tubes under external pressure for $\overline{a} = 0.4$ and $n = -0.430149$ using m as a parameter

Fig.3.20 shows the variation of the elastic limit external pressure with the inner radius a for different m and n values for an FGM tube with fix ends.

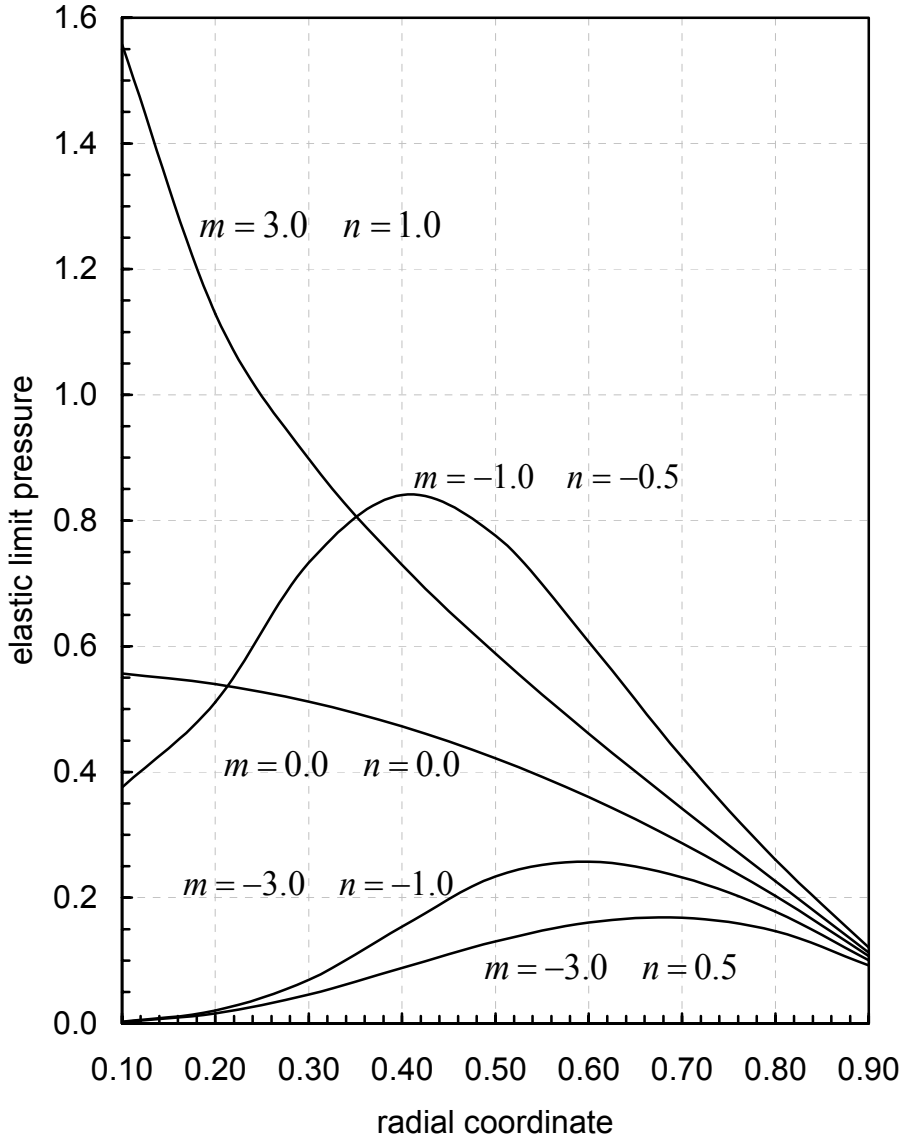

Figure 3.20 Variation of elastic limit external pressure $\overline{P}_e$ with inner radius a using n and m as parameters for the FGM tube with fixed ends

CHAPTER IV

SUMMARY AND CONCLUSION

In this study, the analytical solution of the pressurized functionally graded tube problem is presented. The expressions of the stresses and displacement for the tube assembly are derived first. Using these expressions obtained for different end conditions, the yielding behaviour of the FGM tubes are investigated considering von Mises yield criterion. Several numerical examples are handled in order to show the yielding behaviour of the FGM tubes. In the analyses, four different cases are investigated:

1. Free ends-internal pressure
2. Free ends-external pressure
3. Fixed ends-internal pressure
4. Fixed ends-external pressure

The analyses reveal that, for all cases stated above, depending on the FGM parameters the tubes yield

1. at the inner surface of the tube (at $r = a$) first,
2. at the outer surface of the tube (at $r = b$) first or
3. simultaneously at both locations $r = a$ and $r = b$.

In order to determine the effect of the FGM parameters on the yielding behaviour, a number of parametric analyses are performed. Studies show that the location of the

yielding in an FGM tube may change as the FGM parameters n and m change. By using the analytical solutions given in this study, one can find

a. the location of the yielding at the tube,
b. the corresponding elastic limit pressure, and
c. distributions of stresses and displacement in the FGM tube.

These findings can be used for the analysis and design of FGM tube assemblies. Studies also show that the more advantageous case for the FGM tubes is the simultaneous yielding at inner and outer surfaces, as the elastic limit pressure is maximum for this case. For instance, for a fixed ended FGM tube under external pressure with $a = 0.4$ and $b = 1.0$, the yielding begins at the inner surface for the parameters $n = -0.430149$ and $m = 2.0$. The dimensionless elastic limit external pressure is obtained as $\overline{P}_e = 0.40$ for this case. The dimensional value of this pressure is calculated as 27.52 MPa by the expression in Eq.(33) and

$$P = \overline{P}_e \cdot \sigma_0(a). \tag{41}$$

where $\sigma_0(a)$ is given in Eq. (33). The yielding that begins at the outer surface is considered next. For the FGM parameters $n = -0.430149$ and $m = -2.0$ the dimensionless elastic limit external pressure that cause yielding at $r = b$ is obtained as $\overline{P}_e = 0.33$, which corresponds to a dimensional pressure of 141.90 MPa. On the other hand, for the yielding that begins simultaneously at both surface with the parameters $n = -0.430149$ and $m = -1.78367$, the dimensionless elastic limit external pressure is obtained as $\overline{P}_e = 0.4$ which corresponds to a dimensional pressure of 172 MPa. As seen from these results, the FGM tube which has the highest elastic limit pressure is the one that yields at both ends at the same time.

This study is based on the solution of the pressurized FGM tubes in elastic stress state. For future studies, the elastic-plastic solution of this problem can be studied. In addition, the other material properties such as Poisson's ratio could be considered to have a variable profile.

REFERENCES

[1] Rooney F., Ferrari M., Tension, bending, and flexure of functionally graded cylinders, International Journal of Solids and Structures 38, 413-421, 2001.

[2] Watanabe S. , Ishikura T., Tokumura A., Kim Y. , Hayashi N., Uchida Y., Higa S., Dykes. D., Touchard G., The use of a functionally graded material in the manufacture of a graded permittivity element, Functionally Graded Materials, 373-378, Elsevier Science B.V., 1997.

[3] Katakam S., Krishna D.S.R., Kumar T.S., Microwave processing of functionally graded bioactive materials, Materials Letters 57, 2716–2721, 2003.

[4] Noguchi T., Takahashi K., and Masuda T., Trial manufacture of functionally graded Si-Ge thermoelectric material, Functionally Graded Materials, 593-598, Elsevier Science B.V., 1997.

[5] Esteban S.L., Bartolome J.F., Pecharroman C., Moya J.S., Zirconia/stainless-steel continuous functionally graded material, Journal of the European Ceramic Society 22, 2799−2804, 2002.

[6] Kobayasi H., Fabrication of PSZ-SUS 304 functionally graded materials , Functionally Graded Materials, 209-214, Elsevier Science B.V., 1997.

[7] Çetin S., Analytical solution of a crack problem in radially graded FGM, MSc. Thesis, Graduate School of Natural and Applied Sciences of METU, 2007.

[8] Suresh S., Mortensen A., Fundamentals of functionally graded materials, IOM Communications Ltd. Carlton House Terrace London SW1Y 5DB, 1998.

[9] Eslami M.R., Babaei M.H., Poultangari R., Thermal and mechanical stresses in a functionally graded thick sphere, International Journal of Pressure Vessels and Piping 82, 522–527, 2005.

[10] Akış T., Eraslan A.N., Exact solution of rotating FGM shaft problem in the elastoplastic state of stress, Arch Appl. Mech 77, 745–765, 2007.

[11] Dai H.L., Fu Y.M., Dong Z.M., Exact solutions for functionally graded pressure vessels in a uniform magnetic field, International Journal of Solids and Structures 43, 5570–5580, 2006.

[12] Zhifei S., Taotao Z., Hongjun X., Exact solutions of heterogeneous elastic hollow cylinders, Composite Structures 79, 140–147, 2007.

[13] Shao Z.S., Mechanical and thermal stresses of a functionally graded circular hollow cylinder with finite length, International Journal of Pressure Vessels and Piping 82, 155–163 , 2005.

[14] Zimmerman R.W., Lutz M.P., Thermal stresses and thermal expansion ina uniformly heated functionally graded cylinder, Journal of Thermal Stresses 22, 177-188, 1999.

[15] Akış T., Eraslan A.N., Plane strain analytical solutions for a functionally graded elastic–plastic pressurized tube, International Journal of Pressure Vessels and Piping 83, 635–644, 2006.

[16] Oral A., Anlas G., Effects of radially varying modulus on stress distribution of nonhomogeneous anisotropic cylindrical bodies , International Journal of Solids and Structures 42, 5568–5588, 2005.

[17] You L.H., Zhang J.J., You X.Y., Elastic analysis of internally pressurized thick-walled spherical pressure vessels of functionally graded materials, International Journal of Pressure Vessels and Piping 82, 347–354, 2005.

[18] Shen H., Functionally graded materials, CRC Press Taylor & Francis Group, 2009.

[19] Delale F., Erdoğan F., The crack problem for a nonhomogeneous plane, Journal of Applied Mechanics 50, 609-614, 1983.

[20] Akış T., Elastoplastic analysis of functionally graded spherical pressure vessels, Computational Materials Science 46, 545–554, 2009.

[21] Akış T., Eraslan A.N., Yielding of long concentric tubes under radial pressure based on von Mises criterion, J. Fac. Eng. Arch. Gazi Univ. Vol 20, No 3, 365-372, 2005.

[22] Akış T., Eraslan A.N., Yielding of two-layer shrink-fitted composite tubes subject to radial pressure, Forschung Ingenieurwes 69, 187–196, 2005.

[23] Eraslan A.N., Apatay T., Analytical solution of nonlinear strain hardening preheated pressure tube, Turkish J. Eng. Env. Sci. 32, 41–50, 2008.

[24] Da Silva V.D., Mechanics and strength of materials, Springer-Verlag, Berlin Heidelberg, 2006.